Ana João
Vicente Correia

Automontagem de péptidos para formação de biomateriais nanofibrais

Peptide self-assembly for nanofibre biomaterials

Universidade de Aveiro Departamento de Química
2013

Ana João Vicente Correia

Automontagem de péptidos para formação de biomateriais nanofibrais

Peptide self-assembly for nanofibre biomaterials

Dissertação apresentada à Universidade de Aveiro para cumprimento dos requisitos necessários à obtenção do grau de Mestre em Bioquímica, ramo de Bioquímica Clínica, realizada sob a orientação científica do Doutor Maxim Ryadnov , Investigador Principal no National Physical Laboratory, Doutor Angelo Bella, Investigador Auxiliar no National Physical Laboratory e Doutor Professor Pedro Domingues, Professor Auxiliar do Departamento de Química da Universidade de Aveiro

I

"Nothing in life is to be feared, it is only to be understood. Now is the time to understand more, so that we may fear less" Marie Curie

III

o júri

Presidente   Prof. Dr.ª Rita Maria Pinho Ferreira
professora auxiliar convidada do Departamento de Química da Universidade de Aveiro

Prof. Dr. Pedro Miguel Dimas Neves Domingues
professor auxiliar do Departamento de Química da Universidade de Aveiro

Dr. Maxim Ryadnov
investigador principal no National Physical Laboratoy – United Kingdom

Dr.ª Alisa Rudnitskaya
investigadora auxiliar do Departamento de Química da Universidade de Aveiro

Dr. Angelo Bella
investigador auxiliar no National Physical Laboratoy – United Kingdom

Acknowledgments

I would like to express my sincere gratitude to my supervisor Dr. Max Ryadnov from the National Physical Laboratory for all the help and support given during my research for this thesis. I extend my thanks also to my co- supervisor Dr Angelo Bella who expertise was indispensable to the outcome of this work. I am also extremely grateful to Professor Pedro Domingues from Aveiro University for invaluable help throughout this endeavour. I would also thanks to Lloyd Ryan for his patience when helping me with the set-up process in the laboratory.

Thanks to Adelina Pereira for edited this thesis.

A word of gratitude to my friend Fátima Santos for being there for me when the going got tough.

Thanks to my parents, Armando Correia and Armandina Correia and my sister Tatiana Correia for their unequivocal support and loving.

Last but not least, my most thanks to Pedro Filipe for his unfaltering support. I could not have it without him.

palavras-chave   Biomateriais, péptido-amfifílico, auto-montagem, regeneração de tecidos

resumo   Ao longo da última década, o processo de auto-montagem peptídica têm suscitado considerável interesse pela sua capacidade de gerar novos biomateriais com diversas aplicações, incluindo a regeneração de tecidos e cosméticos. Biomateriais com base peptídica são agrupados de baixo para cima a partir de pequenos blocos de construção. O presente estudo concentra-se na utilização de diferentes motivos estruturais peptídicos para a construção de biomateriais fibrosos. Neste trabalho, diferentes péptidos amfifílicos foram sintetizados utilizando o processo de síntese peptídica do estado sólido para formar distintas estruturais peptídicas. A capacidade de auto-montagem e propriedades biológicos foram caracterizados utilizando dicroismo circular, espectroscopia, microscopia electrónica de transmissão e determinada a concentração mínima inibitória. Os espectros de dicroísmo circular revelaram bobina aleatória e conformações β-folha para as estruturas amfifílicas. A maioria das imagens de TEM revelou estruturas fibrais à nanoescala e foi observada alguma atividade antimicrobiana. Efetivamente, os resultados demonstram que os péptidos sintetizados possuem capacidades de auto-montagem para formarem supraestruturas nanofibras, não revelando no entanto fortes propriedades antimicrobianas. Este trabalho apresenta novos designs de biomateriais com potenciais aplicações em reparação de tecidos através da capacidade de formação de nanofibras

keywords

Biomaterials, peptide-amphiphile, self-assembly, tissue regeneration

abstract

Over the last decade self-assembling peptide systems have attracted considerable interest as novel biomaterials for use in different applications including tissue regeneration and cosmetics. Peptide-based biomaterials are assembled from small building blocks from the bottom up. This study is focused on the use of different peptide folding motifs as building blocks for the construction of fibrous biomaterials. Different peptide amphiphiles (PAs) were synthesized using solid phase synthesis and their folding, self-assembly and biological properties were characterized using circular dichroism (CD) spectroscopy, transmission electron microscopy (TEM) and minimal inhibitory concentration (MIC) assays. CD spectra showed random coil and β-sheet conformations for the amphiphiles. TEM revealed nanoscale fibre structures for most of the PA's, some of which displayed antimicrobial activity. Effectively, the results demonstrate that the designed peptide self-assembles into nanofibre suprastructures. However, the peptides were not strongly antimicrobial and formed fibrillar structures. This work introduces new biomaterial designs with potential applications as nanofibre scaffolds for tissue engineering.

Table of contents

Ackonwledgments
Resumo
Abstract
Table of contents
Table of figures
Table of abbreviation

Table of figures

Figure 1.13: a) The peptide sequence of SAF-p1 and SAF-p2a comprised of two blocks each. A and B blocks for SAF-p1 and C and D blocks for SAF-p 2a. b) B complements C and A complements D. This connection results in a sticky-ended dimer.

Figure 1.14: The discontinuous design of a) CC^{NN} and b) DD^{CC} peptide. β-alanine causes a kinked structure rather than a straight one because of the flexibility induced by this residue.

Figure 1.15: TEM of a) Straight fibres formed between SAF-p1 and SAF-p2a in 1:1 ratio. b) Fibres formed by adding CC^{NN} peptide to SAF-p1/SAF-p2a in 1:1:1 ratio. c) Fibres formed by adding DD^{CC} peptide to SAFp1/SAF-p2a in 0,01:1:1 ratio.

Figure 1.16: Chemical structure of peptide-amphiphile. Region 1 is a hydrophobic segment with 16 carbons. Region 2 consists of four consecutive cysteines. Region 3 is a flexible linker with 3 glycines. Region 4 is a single phosphorylated serine. Region 5 shows the cell adhesion ligand (RGD).

Figure 1.17: Self-assembly of PA in the form of a cylindrical micelle.

Figure 1.18: Sequence of PA1. The molecule includes a hydrophobic region (C_{16}), a glycine region and a charged headgroup.

Figure 1.19: a) Cryo-TEM Images of PA1. This peptide-amphiphile forms nanofibres. b) PA 9 with N-methylated glycine in position 1. This peptide-amphiphile forms spherical micelles.

Figure 2.1: Solid Phase Peptide Synthesis. The green square is a temporary protecting group of an amino group, X, Y and Z are side chains and the red circle depicts a side chain protecting group.

Figure 2.2: Occurrence of polymerization between styrene and DVB.

Figure 2.3: Synthesis of MBHA resin.

Figure 2.4: Deprotection process using TFA.

Figure 2.5: Hydroxybenzotriazole and derivative additive (top) and uronium salts (below).

Figure 2.6: MALDI-TOF with reflectron.

Figure 2.7: CD instrumentation.

Figure 2.8: Representative CD spectra for α-helix (blue line), β-sheet (red line) and random coil (black line).

Figure 3.17: CD spectra at 20ºC for peptide AC8 at 50 μM (black line), 100μM (red line), 200 μM (blue line)

Figure 3.18: CD spectra at 20° C for peptide AC9 at 50 μM (black line), 100μM (red line), 200 μM (blue line)

Figure 3.19: Negatively stained transmission electron micrographs of peptide AC6 (top) and peptide AC7 (below). Assembly conditions in 10 μM MOPS at pH 7.4 left overnight at 20° C.

Figure 3.20: Negatively stained transmission electron micrographs of peptide AC8 (top) and peptide AC 9 (below). Assembly conditions in 10 μM MOPS at pH 7.4 left overnight at 20° C.

Table of abbreviation

ESE - European Society for Biomaterials

FACIT - fibril associated collagens

TEM - Transmission Electron Microscopy

SAF - self-assembling fibers

PA - peptide-amphiphile

CD - circular dichroism

FT-IR - Fourier transform infrared spectroscopy

PA – Peptide – amphiphile

MOPS - 3-(N-morpholino)propanesulfonic acid

DIPEA – dilauryphosphatidyglycerol

EDT – 1,2-Ethanedithiol

HCTU–(2-(6-Chloro-1H-benzotriazole-1-yl)-1,1,3,3-tetramethylamininum hexafluorophosphate)

HBTU - O-Benzotriazole-N,N,N',N'-tetramethyl-uronium-hexafluoro-phosphate

TBTU - O-(Benzotriazol-1-yl)-N,N,N',N'-tetramethyluronium tetrafluoroborate

RP HPLC – Reverse Phase- High Performance Liquid Chromatography

MS – Mass Spectrometer

MALDI ToF – Matrix assited laser desorption ionization time- of- fight

MIC – Minimal inhibitory concentration

Pbf – 2,2,4,6,7-pentamethylbenzofuran-5-sulfonyl

TFA- trifluoroacetic acid

TIS – triisopropyl silane

SPPS – Solid Phase Peptide Synthesis

PEGA - Polyethylene Glycol Polyacrylamide

CLEAR - cross-linked ethoxylate acrylate

PEG - polyethylene glycol

DVB – divinylbenzene

DMF- dimethylformamide

DMC – dichloromethane

MBHA – methylbenzhydrlamnine

Fmoc - 9H-fluoren-9-ylmethoxycarbonyl

Boc - tert-butyolxycarbonyl

HOBt – Hydroxybenzotriazole

HOAt - 1-hydroxy-7-azabenzotriazole

UV – ultraviolet

TCEP - *tris*(2-carboxyethyl)phosphine

Chapter 1 - Introduction

1.1 - Biomaterials

In 1976, the European Society for Biomaterials (ESE) defined a biomaterial as "a nonviable material used in a medical device, intended to interact with biological systems" (1, 2). However, the current definition put forward for a biomaterial is "a material intended to interface with biological systems to evaluate, treat, augment or replace any tissue, organ or function of the body (3 ,4). Biomaterials have been investigated because of their many potential biological functions, such as releasing polypeptide growth factors, blocking antibody permeation and serving as matrices to guide tissue regeneration (3,5).

Biomaterials have become a promising area of research with successful applications in medicine and bioengineering (6). Different chemical systems have been developed as biomaterials, including synthetic polymers, and recently, molecular design based on biological structure. Polymeric biomaterials with inorganic systems have been used in tissue engineering, particularly in orthopaedic research (7). Hydrogels differ from most biomaterials as they do not dissolve in water and have also found use for biomedical applications (3).

1.2 - Peptide-based biomaterials

Complementary strategies can be used in the fabrication of molecular biomaterials. These materials can be generated by stripping down or molecule-by-molecule assembly (5, 6). However, molecular self-assembly is considered to be the most powerful approach in the fabrication of novel materials. Peptides self-organize to form a distinct structure with a specific functionality (8). For this reason, this process has been exploited for the production of synthetic material where proteins are versatile building blocks for fabricating materials.

Much research has been focused on self-assembling peptides that produce supramolecular structures with very distinct features. Different structural motifs can be used as self-assembling building blocks. For example, α-helix, β-sheet, collagen and amphiphilic peptides have been shown to give different supramolecular morphologies (Figure 1.1). Other examples include ionic self-complementary peptides, which is a type of surfactant-like peptide, surface nano-coating peptides and molecular switches (6). All these structures can be cross-linked together to form fibrous structures.

α-helical structure	β-structure	Collagen Structure	Amphiphilic structure
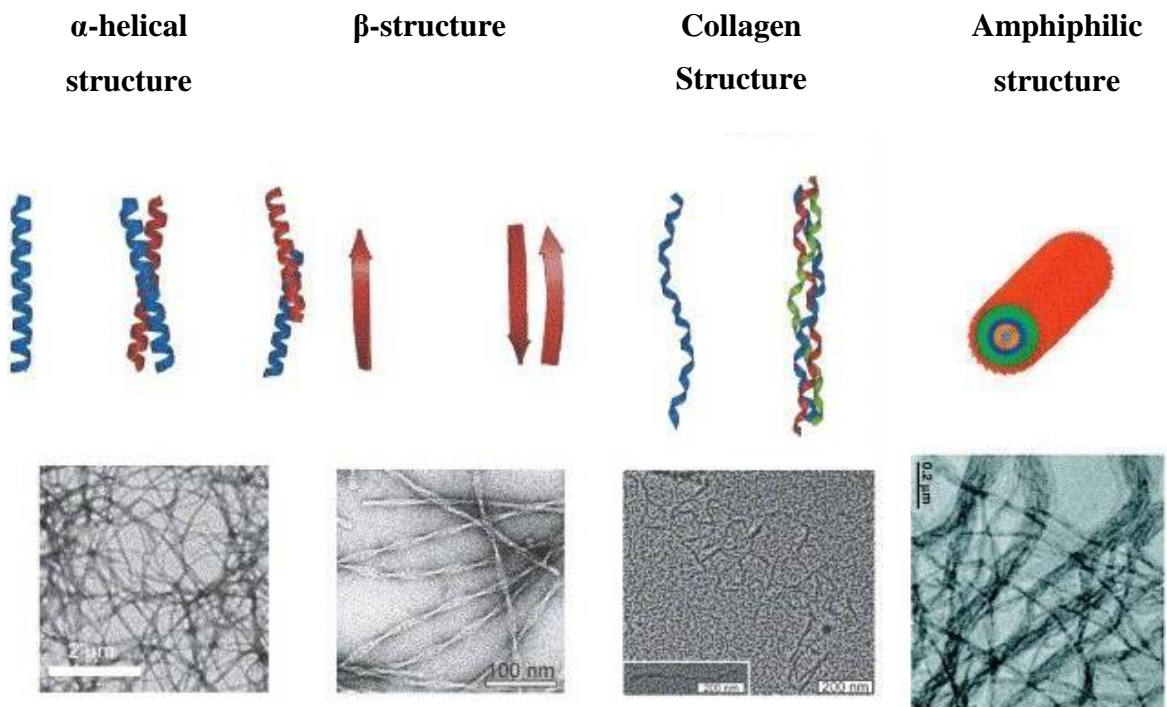
Figure 1.1: Examples of protein structural motifs, schematics (top) and transmission electron micrographs (bottom) (6).

Biomaterials play an important role in many activities, for example, as matrices to guide tissue repair, and in the stimulation of a vascularization response releasing growth factors (9). In the future biomaterials will assume an important role in medicine and be used in a wide variety of non-medical applications through biological design and the incorporation of dynamic behaviour (10). For these reasons the study of these peptide-based materials is a promising field of research and of interest for use in the fabrication of different materials for a wide range of applications.

1.3 – Peptide self-assembly

1.3.1- Features of peptides used as building blocks

The molecular arrangement of peptide materials has been investigated over the past years (10). Their molecular structures may be constituted by biological, organic and/or inorganic compounds (10). For this reason, understanding molecular structure is a crucial step when building a new biomaterial.

Self-assembly is a process in which biological entities (building blocks) are spontaneously organized to form a supramolecular structure (11, 12). However, this mechanism displays special interactions that enable the construction of a novel material (13). The driving forces of molecular self-assembling are non-covalent interactions, such as hydrophobic, ionic, Van der Walls forces and hydrogen bonds, which are essential for the specific association between different building blocks. Among the building blocks used are short peptides (12).

Peptides are polymers of α-amino acids connected through peptide bond (amide bond) (Figure 1.2b) (8). The bond formation occurs between the carboxyl and the amide group present in all natural amino acids. An amide bond is formed between two amino acids through the release of a water molecule where the α-carbon is a chiral centre asymmetric (Figure 1.2a) (8). What characterizes each of these molecules is the variable group R side chain, which provides different properties and biological functions. In nature there are 20 amino acids. These are divided into polar and non-polar structures, as well as according to charge (positive or negative) (8).

a)

b)
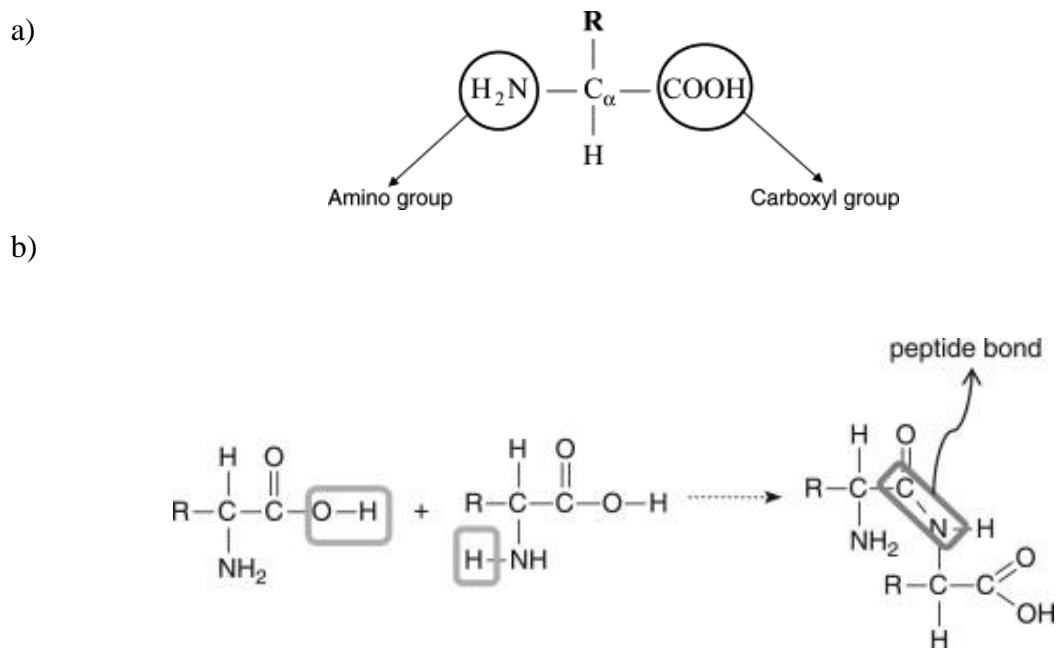
Figure 1.2: a) Schematic representation of amino acids. R is the side chain specific to each amino acids (2) b)Peptide bond (amide bond) between two amino acids (2). The amide bond is a chemical covalent bond that results from the reaction between the carboxyl group of an amino acid and the amine group of another.

1.3.2- Protein folding motifs

1.3.2.1 –α-helix and β-sheet

The mechanism by which the protein folds to form different structures is not yet fully understood (14, 15). Knowing how the amino acid sequence interacts to form a 3-D structure is a crucial to understanding their contribution to the protein folding process (16) There are two main folding motifs in proteins: α-helices and β- sheets (17).

The α-helix structure is characterized by hydrogen bonds between the N-H group of an amino acid (α) and its C=O group (i +4, i+7), as seen in figure 1.3. Generically, it could be described as the coiling of the amino acid sequence around a

virtual axis. Experimental measurements indicated a periodicity of 3.6 amino acids per helical turn (figure 3) (18).

a)   b)
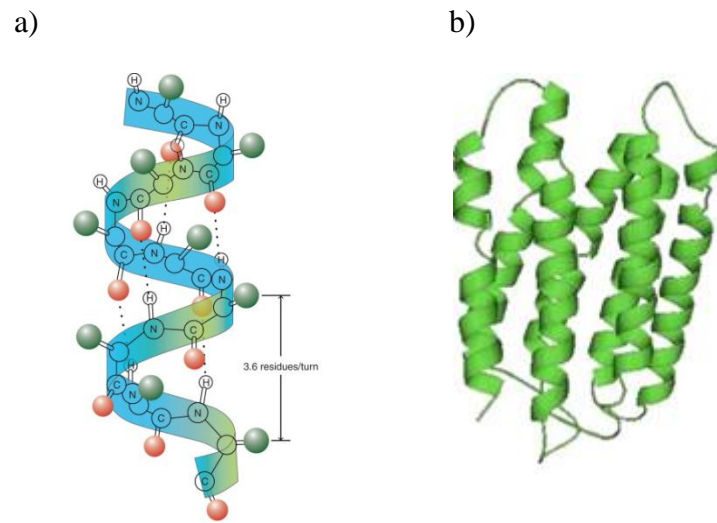
Figure 1.3: a) Structure of α-helix display the hydrogen bond between N-H group and CO group. Representation of 3.6 residues per turn (3) . b) Model protein classes (16).

The β-sheet structure consists of different β-strands laterally connected by hydrogen bonds between their NH and C=O groups along the peptide/protein backbone- (19). The type of arrangement and relationship between the sequential strands is defined by hydrogen bonds. In a parallel arrangement, all strands are oriented in the same direction (Figure 1.4). However, when the orientation of the strands is opposite an antiparallel β sheet is formed (Figure 1.4) (19). The torsion angles that β-sheet can adopt depend on the type of the side chain formed by amino acid residues.

The formation of parallel β sheet in protein aggregation is associated with some neurodegenerative diseases like Alzheimer's, Parkinson's and prior disease (19, 20). Many researchers have sought to understand the factors that lead to amyloid formations, such as protein sequence and environment conditions. Other studies have focused their investigation on the variety of β-sheets that derive from amyloid protein (21).
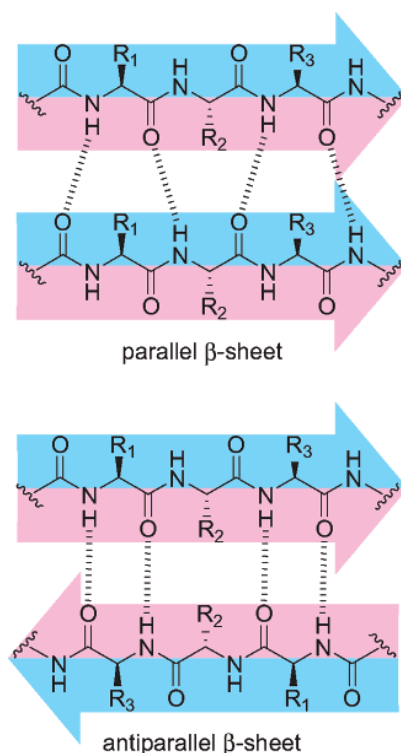
Figure 1.4: Structures of parallel and anti parallel β-sheet which show the difference in hydrogen bond patterns. (19)

The secondary structure of peptide molecules has gained considerable interest among researchers who work in the field of self-assembly (21). The β-sheet can be a fundamental element of a building block for nanomaterials using proteins (22). Consequently, the importance of this secondary structure is currently being investigated due to its potential for the development of a new structure design for various applications. Lorraine *et al* studied four peptides and have proposed designs that bring about the formation of β-sheet at the air-water interface (23). They quantified the intermolecular interactions that take place between phase behaviours, which allowed these researchers to explore the relationship of self-assembly and its role in the production of composite biomaterials (23).

Matthew *et al*, on the other hand, have designed a new peptide with two β-sheets containing hydrophobic valine and hydrophilic lysine residues in alternation (14). The central sequence contains diproline translated as Pro-Pro, which opens up conformation and supports *trans* linkage. The ^DPro-^LPro sequence undergoes intermolecular folding and adopts a β-hairpin conformation, which self-assembles as

β-sheet-rich hydrogels. Contrarily, peptide with an ^{L}Pro-^{L}Pro sequence adopts an extended β-strand and self-assembles as amyloid fibril. Figure 1.5 shows both folded peptides along the fibril axis translated as formation of intermolecular β-sheet hydrogen and extended β-strand. These structures exhibit characteristics similar to those of amyloid fibril, which, when assembled, are stable at different Ph levels and temperatures (14).
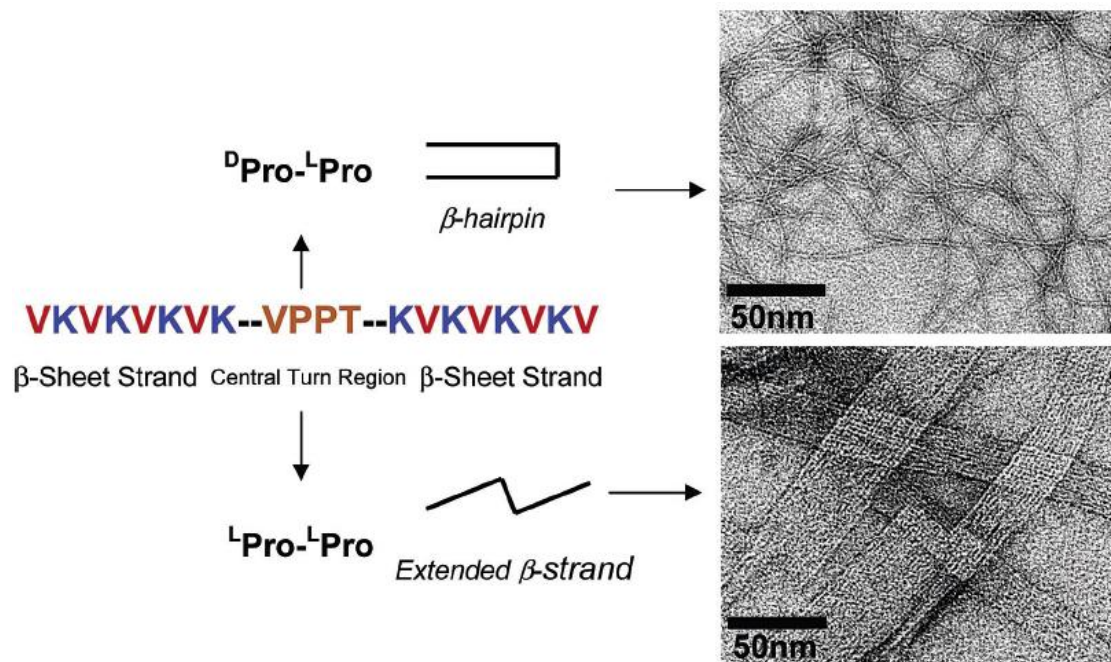
Figure 1.5: The peptide sequence and self-assembled material. Peptides with ^{D}Pro-^{L}Pro adopt β-hairpin conformation and TEM revealed entangled fibrils with a widhth of 3 nm each. Peptides with ^{L}Pro-^{L}Pro adopted extended β-strand conformation and TEM revealed fibrils (14).

1.3.2.2 – Collagen

Collagen, which exhibits very characteristic folding, is the most prevalent protein in the animal kingdom (24). This protein is located at diverse sites with specific functions, playing a key role in maintaining tissue and cellular size and shape (25). Because of this key structural feature, collagens have acquired significant interest within the scientific community (26).

The structure of collagen was determined by X-Ray diffraction over 50 years ago. It is characterized by a triple helix with three different polypeptide chains (α-helix) that are combined to fold together to the left (27,29). Amino acid composition consists of a repeated tripeptide with a X Y Gly sequence, in which Proline (Pro) and hydroxyproline (Hyp) are predominant in the X and Y positions, respectively (Figure 1.6) (28, 30). The latter amino acids (Pro and Hyp) help to stabilize the triple helix, while glycine (Gly) facilitates hydrogen bonding and intermolecular cross-link.

a)   b)
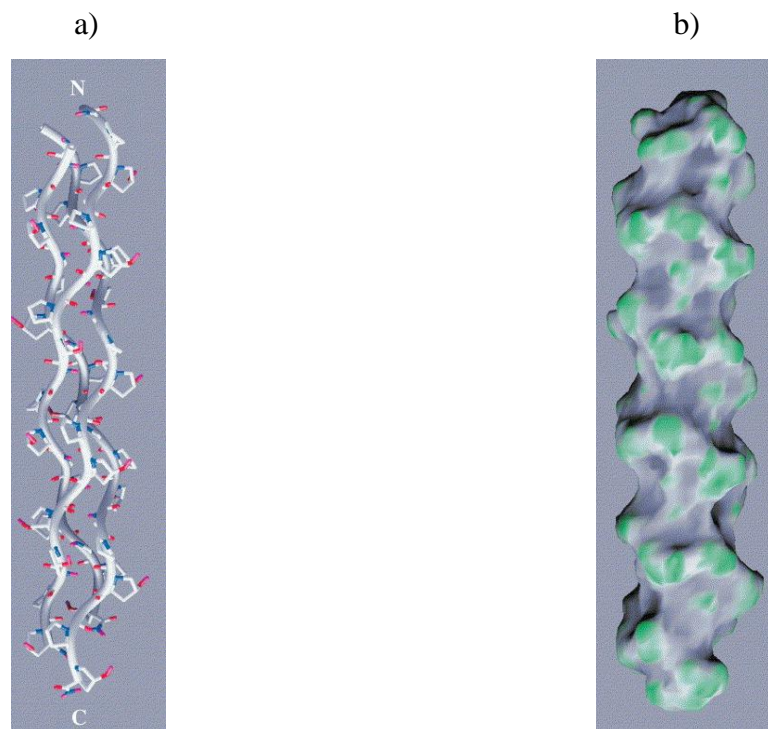
Figure 1.6: a) Molecular structure of collagen - like peptide (Ac-Pro-Hyp-Gly-HH$_3$) triple helix (28). b) The molecular surface (28)

The collagen self-assembly has not been fully understood, but several methods describe this process like a periodic fibrilar assembly (31). Some studies have indicated that fibers consist in building blocks with periodicities (29). Three peptide chains forming the triple helical collagen molecule of 294, 8 nm in length and 1,5 nm in diameter (24). Hydrophobic and electrostatic interactions are involved in the arrangement of the collagen monomers where several molecules form a microfibril. These microfibrils have been suggested that to be the building blocks of fibril with a

67 nm (D-period) periodicity axial (24). The figure 1.7 shows the hierarchical organization of collagen.
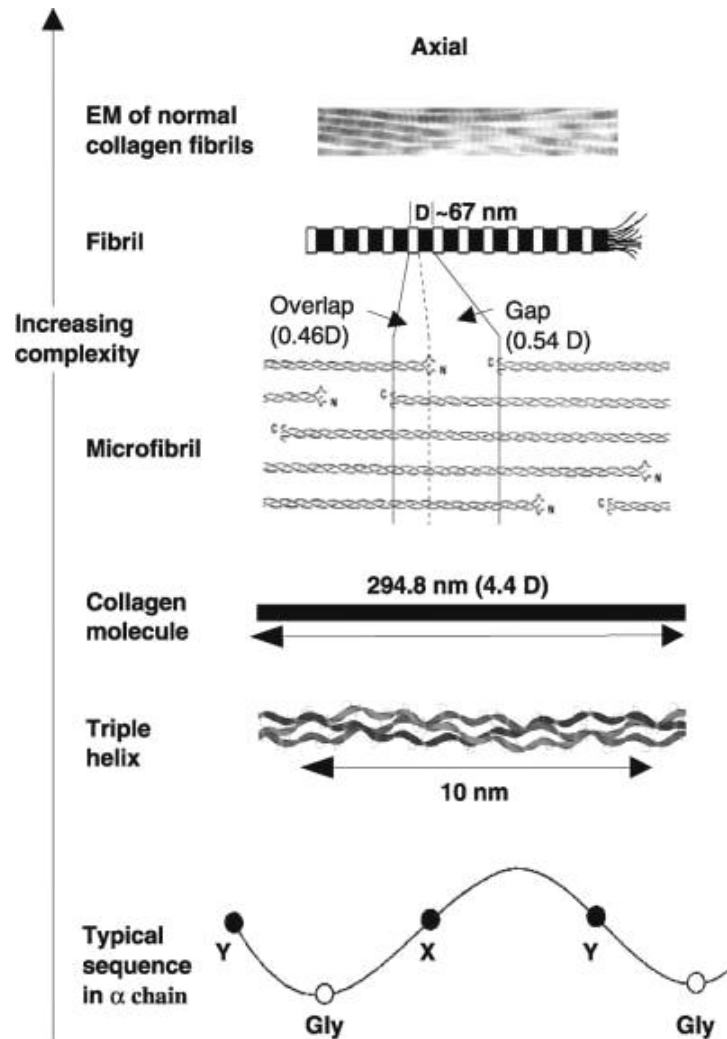
Figure 1.7: Structural Hierarchy of Collagen (29).

Nearly 30 types of collagen proteins were identified and described with different structures, organization and localization (30). These are characterized by a complex structure, splice variants, self-assembly ability and several biological functionalities. Collagen can be classified as fibril-forming collagens, microfibrillar collagens, anchoring fibrils, hexagonal network forming collagens, fibril associated collagens (FACIT), transmembrane collagens and multiplexins (31).

Rele *et al* have described the solid phase synthesis of collagen-mimetic triple helix peptide promoters (32). According to these authors, the primary sequence

comprises three different X Y Gly domains, where the Pro-Hyp-Gly central core is flanked with Glu (negative charged) or Arg (positive charged) peptide repetition (Figure 1.8a). The presence of strong electrostatic and hydrogen bonds between staggered positions allows the formation of thermodynamic stable complexes (Figure 8b).

a)

HN-Pro-Arg-Gly-Pro-Arg-Gly-Pro-Arg-Gly-Pro-Arg-Gly

Gly-Hyp-Pro-Gly-Hyp-Pro-Gly-Hyp-Pro-Gly-Hyp-Pro

Glu-Hyp-Gly-Glu-Hyp-Gly-Glu-Hyp-Gly-Glu-Hyp-Gly-COOH

b)
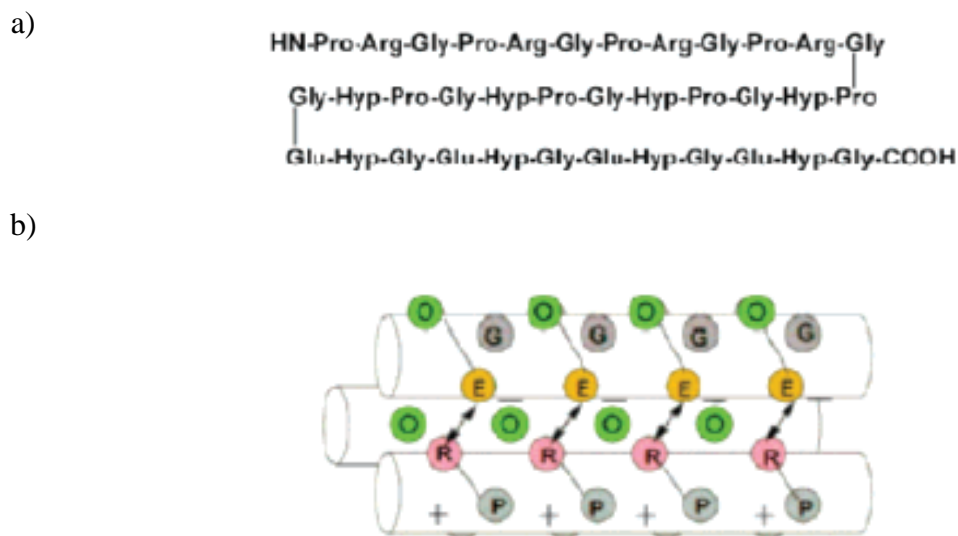
Figure 1.8: a) Amino acid sequence of collagen-mimetic peptide indicating the distinct domains found in its structure. b) Interhelical electrostatic interactions yielding triple-helical protomers (32).

Figure 1.9 shows a Transmission Electron Microscopy (TEM) image of a synthetic peptide which was self-assembled into a periodic fibrous structure. After a long period of incubation the formation of ~70 nm diameter uniform micron-length fibres was observed. The capacity to design periodic elements into reliable assemblies can facilitate fabrication and tailored ordered materials for several applications.
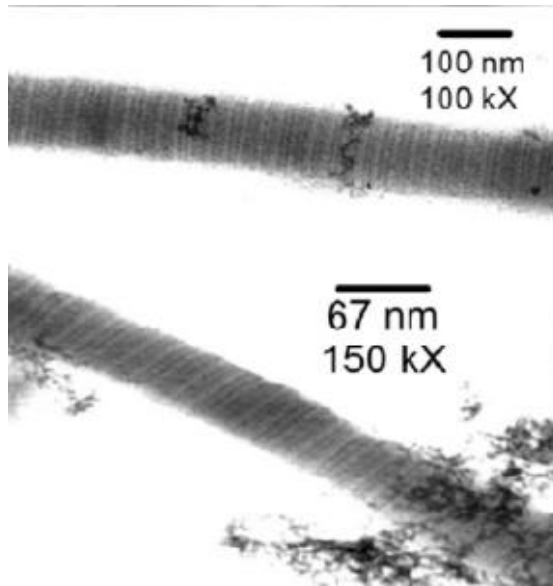
Figure 1.9: High magnification transmission electron micrographs reveal a well defined periodic structure (32).

1.4– α-helix and coiled coil–based biomaterials

In reality, the coiled coils domain is present in several proteins that play important biological functions. The examples of these proteins are transcription factors, muscle myosin, tumour suppressors and cytoskeleton proteins. For this reason, coiled coil domains have attracted special interest for use in the design of new synthetic peptides.

1.4.1 –Design principles

The coiled coil structure was originally observed in native proteins (33). This structure consists of two or more α-helixes that are wound into a superhelix (34, 35). Coiled coil is characterized by the distance of a full-turn of the superhelix ("pitch"), by the angle between the helix and its axis ("pitch angle") and the angle between two neighbouring helices ("helix-crossing angle") (36). Figure 1.10 shows the global parameters of a coiled-coil.
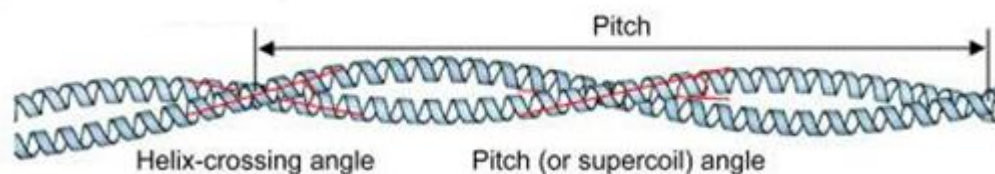
Figure 1.10: Global parameters of a coiled-coil structure [37].

Usually α-helix requires 3.6 amino acids per turn. However, a coiled coil helix shifts to the left and accommodates 3.5 residues per turn (18). This allows the repetition of side chains after every sequence of seven residues. The design of coiled coil peptides is based on heptad repeats. The heptad amino acids are also named *abcdefg,* where *a* and *d* are hydrophobic, *e* and *g* are positions often occupied by charged amino acids, and the remaining amino acids are generally hydrophilic residues (35, 36). Hydrophobic residues have an important role in structure stability during the self-assembly process, forming the helix interface, while the amino acids in *e* and *g* positions allow electrostatic recognition (33).

The α-helices can be combined to form parallel or antiparallel homodimers or heterodimers. (34). The orientation of coiled coil helices is determined by the interaction between the two heptads residues (33). Figure 1.11 shows amino acid repetition and illustrates the two different orientations that can be found between α-helix in a coiled coil. In a parallel coiled coil the residues in *d* position of one α-helix interacts with the amino acids of the neighbouring α-helix in the same position. (37). On the other hand, in a antiparallel coiled coil the α-helix runs in the opposite direction to that of a parallel coiled coil, which means that the residues found at *d* position interact with the amino acid found at *a* position. These different orientations have been exploited to design several synthetic peptides.
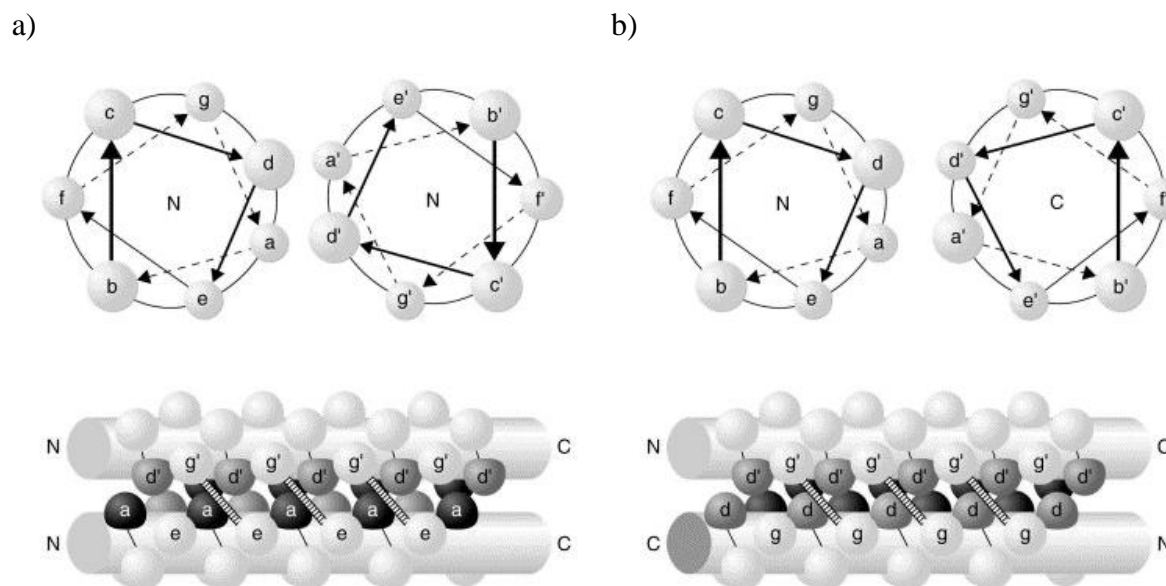
Figure 1.11: Schematic side view representations of two–stranded parallel and antiparallel coiled coils. The residues of one helix are labelled *a-g*, while those of the other helix are marked *a`- g`*. a) Illustration of a parallel coiled coil showing both N termini. Potential interactions between *g´* and *e* residues are indicated. b) Representation of an antiparallel coiled coil where the N termini is shown on the left and C terminus on the right. Potential interaction between *g`* and *g* residues (38).

1.4.2. – Assemblies based on coiled-coil

The success in the development of novel designed molecules from spontaneously peptide-based building blocks has motivated further research in molecular design. The design of a coiled coil covers every type of structure from parallel and antiparallel homodimers to parallel and antiparallel heterodimers (39). Most peptides with self-assembly capacity described in literature use a solid phase peptide synthesis technique as it is very efficient (40, 41). In light of this, some researchers have sought to design α-helix coiled coil with the ability to grow and form fibrous aggregates (42, 43).

Many works suggest that α-helix coiled coil plays an important role in the promotion of peptide self-assembly. Woolfson and co-workers described peptides based on parallel folding of a coiled coil, which allows for the understanding of the

design principles of self-assembly in peptide systems (36, 39). The peptides the authors investigated consisted of heptad repeats with isoleucine and leucine in hydrophobic positions *a* and *d*, respectively. The research group introduced glutamates and lysines in *g* and *d* positions to allow the occurrence of ionic interactions. (Figure1.12). The resulting fibres were straight, rod-shaped and micro in length.
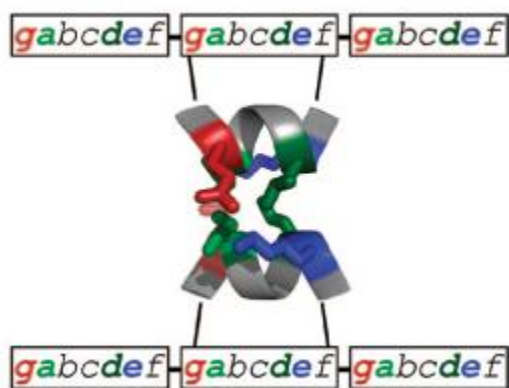
Figure 1.12: Dimeric coiled coil heptad with specific residues at *g, a, d* and *e* positions (36).

Dong *et al* described four coiled coil peptides which are differentiated by the amino acids found at *b*, *c* and *f* positions (44). These particular amino acids were selected with the aim to form a dimeric coiled coil. The researchers demonstrated that nanofibres are formed when the concentration of a peptide increases. In addition, they observed that introduction of positive charge residues at *b*, *c* and *f* positions results in the appearance of nanofibres with diameters of 4 nm. On the other hand, in the absence of positive charge residues self-assembly created fibres 20 or more nanometres in diameter. This observation led to the creation of an alternative mechanism for self-assembly.

In previous works Woolfson *et al* introduced the concept of self-assembling fibres (SAF)(45). This system comprises a design with two complementary *de novo* leucine-zipper peptides that form a sticky ended heterodimer (46). Each peptide is 28 residues-long that assemble and mix to form fibres. The mature SAF samples were

prepared with a mixture of SAF-p1 and SAF-p2 (39). The primary sequence of these is characterized by heptad repeat, HPPHPPP, where H is hydrophobic and P polar residues. Ryadnov *et al* applied the SAF concept to produce heterodimers in a parallel coiled coil (47). SAF peptides have different subunits, namely A and B domains in SAF-p1 and C and D regions in SAF-p2. Thus, A and D regions complement each other, whilst B is complementary to C (Figure 1.13b). In this investigation, SAF-p2 was re-designed as SAF-p2a because the latter interacted better and more efficiently with SAF-p1 (see Figure 1.13a). This combination improved affinity between the two protofibrils, and resulted in the formation of straight fibrils, as shown in Figure 1.15a.
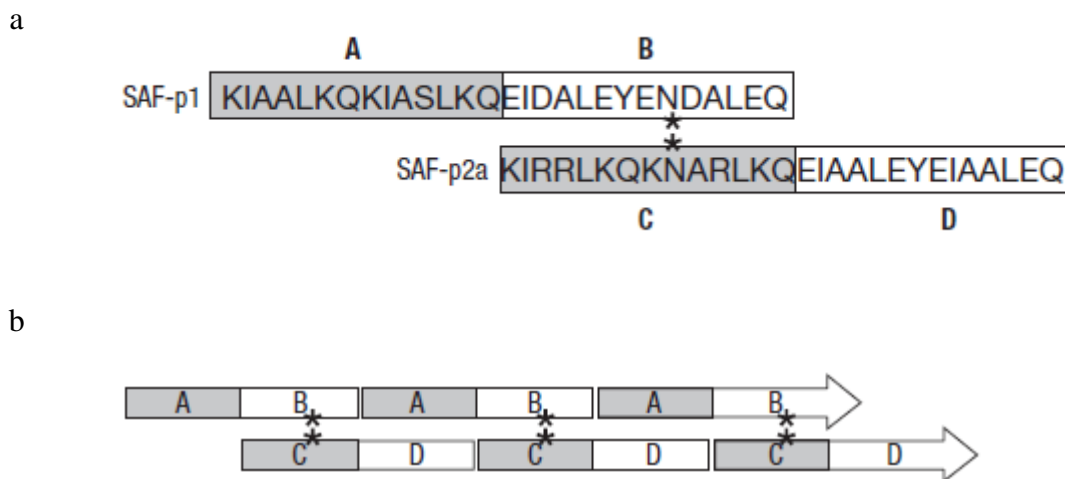
Figure 1.13: a) The peptide sequence of SAF-p1 and SAF-p2a comprised of two blocks each. A and B blocks for SAF-p1 and C and D blocks for SAF-p2a. b) B complements C and A complements D. This connection results in a sticky-ended dimer (47).

Another alternative explored by the authors was the introduction of discontinuities into the SAFs fibres, which brought about kinks and splits in the two new peptides CC ^{NN} and DD ^{CC}, respectively. The CC^{NN} peptide is comprised of two copies of block C linked by the C-termini, while both N-termini remain free. This enabled the interaction between the two blocks. However, the two copies of C blocks are joined by β-alanine to give flexibility to the peptide structure. The DD^{CC} peptide follows a similar principle:

two copies of D blocks are linked via N-termini while C-termini remain free. Figure 1.14 schematically shows the conception of both peptides. Due to differences in their sequence blocks, fibres with distinct characteristics were observed (Figure 1.15).
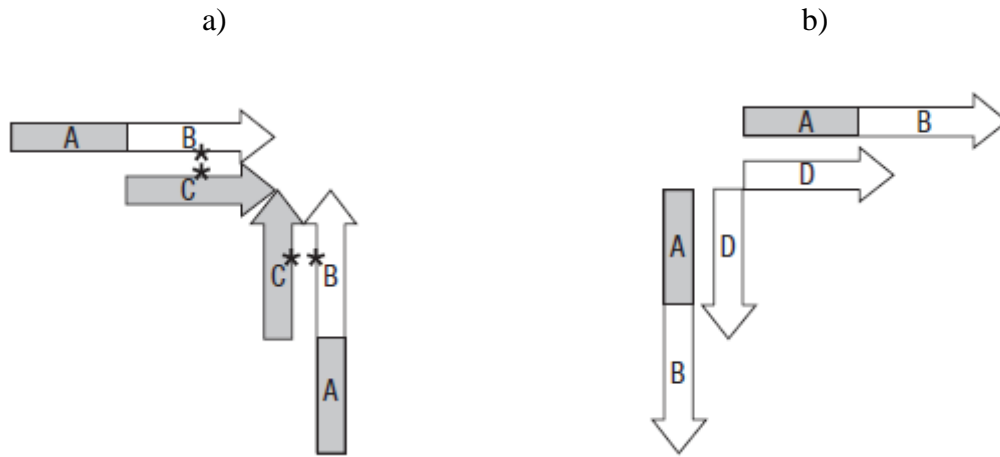
Figure 1.14: The discontinuous design of a) CC^{NN} and b) DD^{CC} peptide. β-alanine causes a kinked structure rather than a straight one because of the flexibility induced by this residue (47).

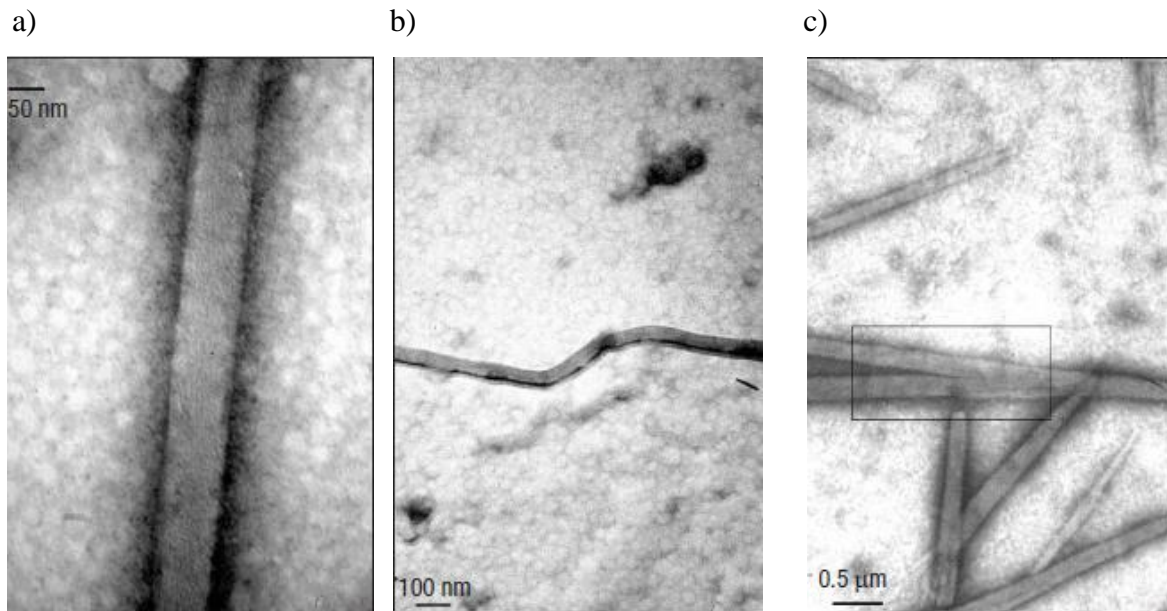**Figure 1.15: TEM of: a) Straight fibres formed between SAF-p1 and SAF-p2a in 1:1 ratio. b) Fibres formed by adding CC^{NN} peptide to SAF-p1/SAF-p2a in 1:1:1 ratio. c) Fibres formed by adding DD^{CC} peptide to SAFp1/SAF-p2a in 0,01:1:1 ratio (47).**

1.5- Peptide-Amphiphile

Amphiphilic molecules are constituted by distinct hydrophobic and hydrophilic segments (48). This structure consists of a peptide attached to a hydrophobic alkyl tail. Aliphatic tails in an aqueous solution tend to aggregate, while the peptide portion packs on the surface. It is well known that self-assembly leads to the formation of nanofibres with a structure similar to that of cylindrical micelles (49). This formation is possible due to a number of interactions like dipole-dipole, hydrogen bond, nonspecific van der Walls interaction and hydrophobic force.

Self-assembly of peptide-amphiphile (PA) has raised interest in scaffolding of new biomaterials for many applications (50). Self-assembled PA can adopt various morphologies by choosing different residues and alkanes. Stupp *et al* have designed a peptide-amphiphile with a hydrophobic tail and a hydrophilic peptide head (Figure 1.16) (51). This peptide was synthesized by standard solid phase chemistry according to the following specific features: 1) four cysteine amino acids were incorporated to form disulfide bonds between adjacent molecules. 2) the serine was phosphorylated at the peptide end to attract calcium and other ions, and to regulate and facilitate the mineralization of hydroxypatite. 3) Arg-Gly-Asp (RGD) sequence was introduced into the peptide to promote cell attachment to the nanofibres. The last of these characteristics would be beneficial for biomedical applications. TEM imaging suggests that assembled peptide-amphiphile forms nanofibres and is stable in an alkaline solution (Figure 1.17).
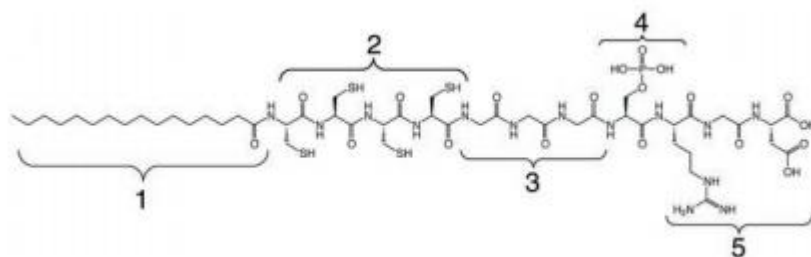
17

Figure 1.16: Chemical structure of peptide-amphiphile. Region 1 is a hydrophobic segment with 16 carbons. Region 2 consists of four consecutive cysteines. Region 3 is a flexible linker with 3 glycines. Region 4 is a single phosphorylated serine. Region 5 shows the cell adhesion ligand (RGD) (51).
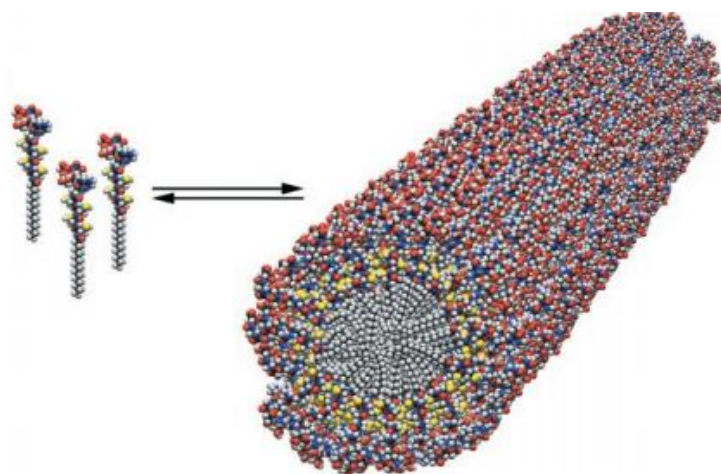
Figure 1.17:Self-assembly of PA in the form of a cylindrical micelle (51).

Later Hartgerink and co-workers reported a prototypic peptide amphiphile containing 12 amino acids and an alkyl tail with 16 carbons (52). The importance of hydrogen bonds in self-assembly was investigated through a set of 26 PA's, including 19 N-methylated variants and 7 alanine mutants. PA1 has a linker region (seven glycines) connecting the hydrophobic segment to the head group, which consists of Glu-Arg-Gly-Asp-Ser (ERGDS) sequence (Figure 1.18). The remaining PA consists of peptides with alanine mutations.
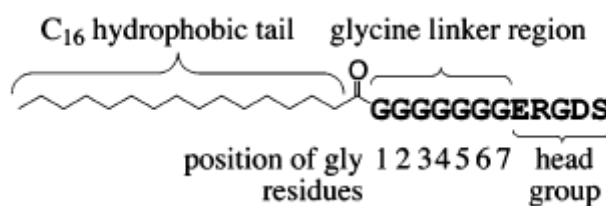
Figure 1.18: Sequence of PA1. The molecule includes a hydrophobic region (C$_{16}$), a glycine region and a charged head group (52).

These peptides displaying alanine mutations were analyzed by circular dichroism (CD), Fourier transform infrared spectroscopy (FT-IR) and TEM. It was found that the four amino acids close to the core are critical for self-assembly of PAs into nanofibres. For this reason, by selectively eliminating the key hydrogen it is possible to change the nanostructure resulting from self-assembly. Thus, this study helps to understand the self-assembly mechanism of peptide-amphiphile.
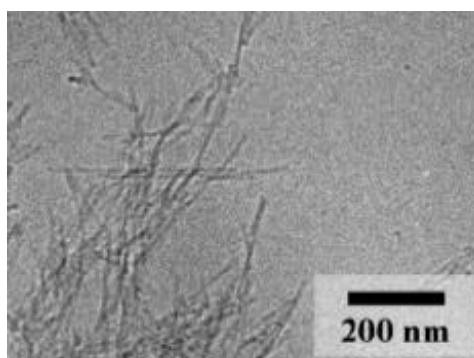
Figure 1.19: a) Cryo-TEM Images of PA1. This peptide-amphiphile forms nanofibres.

1.6 - Aim and objectives

Biomaterials have led to great improvements in many applications due to their specific characteristics. The aim of the present work is to fabricate a new biomaterial with capacity to self-assemble by synthesizing and characterizing a new peptide with different folding.

The specific objectives of this work are:

1. Design and synthesis of a new peptide with different folding using the solid phase peptide synthesis method;

2. Purification using High Performance Liquid Chromatography (HPLC);

3. Biophysical characterization of generated models in aqueous and membrane environments and analysis by circular dichroism (CD)

4. The use of electron transmission microscopy (TEM) to confirm the presence of nanofibres.

5. To investigate the interactions of the synthesised constructs with bacteria

Chapter 2 - Methods and Materials

2.1-Solid Phase Peptide Synthesis

Solid Phase Peptide Synthesis (SPPS) as conceived and demonstrated by Merrifield can provide oligopeptides and small proteins (53, 54). The strategy is based on the use of amino acid side chain protection and the attachment of a C-terminal amino acid to an insoluble polymeric support (i.e. solid) via a linker (55). Side chains that may be reactive and an α-amino group are protected with temporary protecting groups to avoid them reacting with each other (56). The process starts with the coupling of the first amino acid to the resin followed by the deprotection of the α-amino protecting group. After this a second protected amino acid can be introduced in the growing sequence. This cycle is repeated until the required peptide sequence is assembled. At the end of the synthesis, the protecting groups are removed and the bond between the C-terminal amino acid and the polymeric support is cleaved with a specific reagent (56). Figure 2.1 shows the scheme of solid phase peptide synthesis.
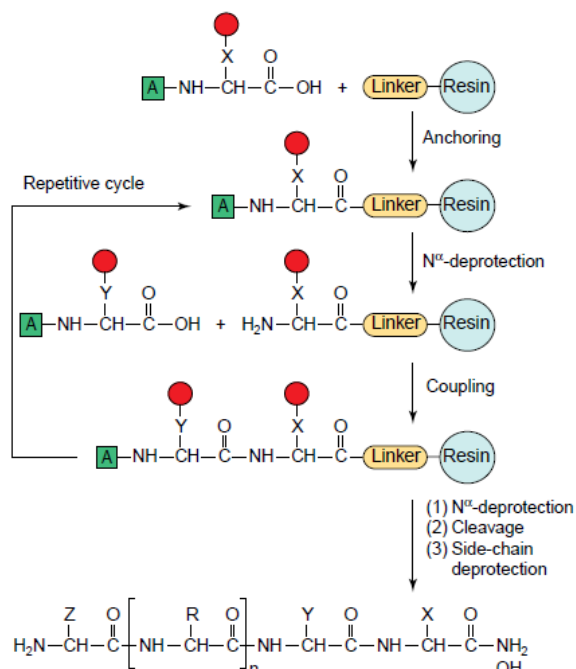

Figure 2.2: Solid Phase Peptide Synthesis. The green square is a temporary protecting group of an amino group, X, Y and Z are side chains and the red circle depicts a side chain protecting group (53).

The main advantage of this method is that there are only two reactions, the amide bond formation and deprotection. These require optimization and the use of excess solvents and reagents, as well as the removal of by-products by simple washing (53,57). On the other hand, SPPS has its limitations, namely the number of peptides achievable is restricted (maximum 50 amino acids) and the fact that the method implies the use of a large quantity of expensive solvents (53).

2.1.1 – Solid Support

Different solid supports have been developed over time. The resins normally used as supports are polyethylene glycol polyacrylamide copolymer (PEGA) resin, cross-linked ethoxylate acrylate resin (CLEAR), polyamide resin and polyethylene glycol (PEG) (58). However, of these the most widely used in solid phase synthesis is a cross-linked polymeric resin obtained from the co-polymerization of styrene and divinylbenzene (DVB) (figure 2.2)(58). Polystyrene is a co-polymer of linear vinyl benzene**.**
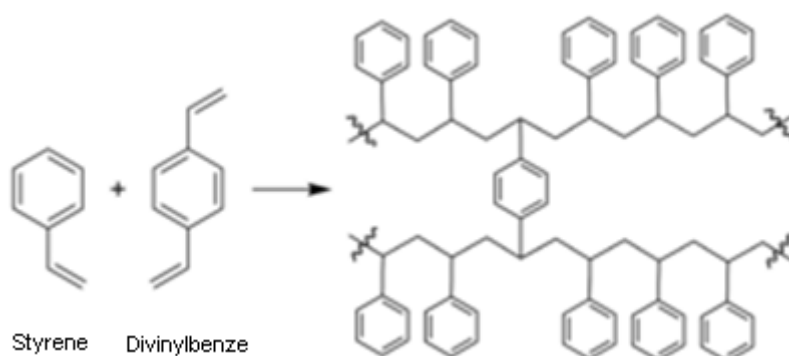

Styrene   Divinylbenze

Figure 3.2: Occurrence of polymerization between styrene and DVB (59).

The quantity of divinylbenzene used for cross-linking is about 1-2% (56). Consequently, this resin has an increased hydrophobicity that can affect the peptide assembly (57).

2.1.2 – Linkers

The choice of linkers depends on the synthesis method used, hence the development of a large number of linkers. Linkers in solid phase synthesis provide an anchor point on the solid support. During peptide synthesis the linker should be stable (60). Among the several linkers used in SPPS, Wang resin is one of the most popular. This is a Merrifield resin with a Wang linker, which results from the reaction between *p*-hydroxybenzyl and methyl-4-hydroybenzoate (61). After coupling, this intermediate is reduced in the ester group by LiAIH$_4$ (61), and at the end of the synthesis the resin is treated in acidic conditions with 95%TFA (trifluoroacetic acid) to cleave the ester linked (60, 61).

MBHA (methylbenzhydrlamnine) resin is used in the synthesis of peptide amides (62). This resin is prepared from *N*-[(benzotriazol-1-yl)(*p*-tolyl)methyl]formamide or *N*-[formamido(*p*-tolyl)methyl]formamide as shown in the figure 2.3(57, 62). Upon completion of synthesis, the peptide is cleaved from the resin by 95%TFA.
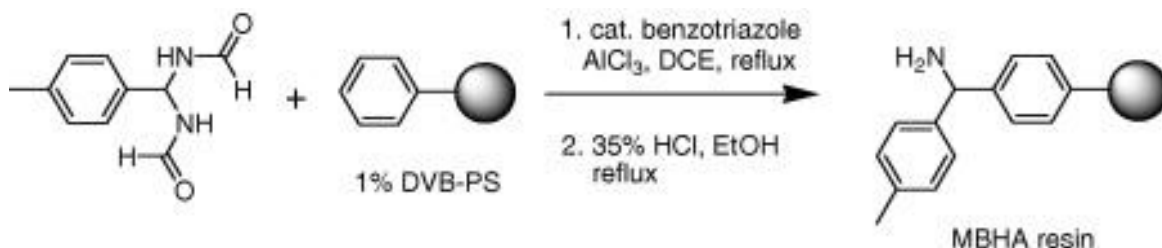

Figure2.4: Synthesis of MBHA resin (62)

2.1.3 – Fmoc and Boc strategy in solid phase peptide synthesis

In amino acids the side chain group, R, defines their structure and properties. Side chains in amino acids can be reactive and may interfere with the formation of the amide bond if not protected. For this reason, protecting groups are necessary for a side chain and an α-amino protection group (56). Fmoc (9H-fluoren-9-ylmethoxycarbonyl) and Boc (tert-butyolxycarbonyl) are two different α-amino protecting groups used in SPPS (56). The choice between Fmoc or Boc depends on the nature of the resin (53, 56). In Fmoc peptide synthesis basic conditions are used to remove the α-amino protecting group after each coupling, but the side chain protecting groups are removed in acidic conditions at the end of the synthesis simultaneously with the cleavage of the resin (56).

The Boc protecting group is removed using strong acids such as TFA. As shown in figure 2.4, tert-butyl carbonium ions are formed during deprotection (57). Fmoc is a base labile group and is removed under strong basic conditions typically using piperidine.
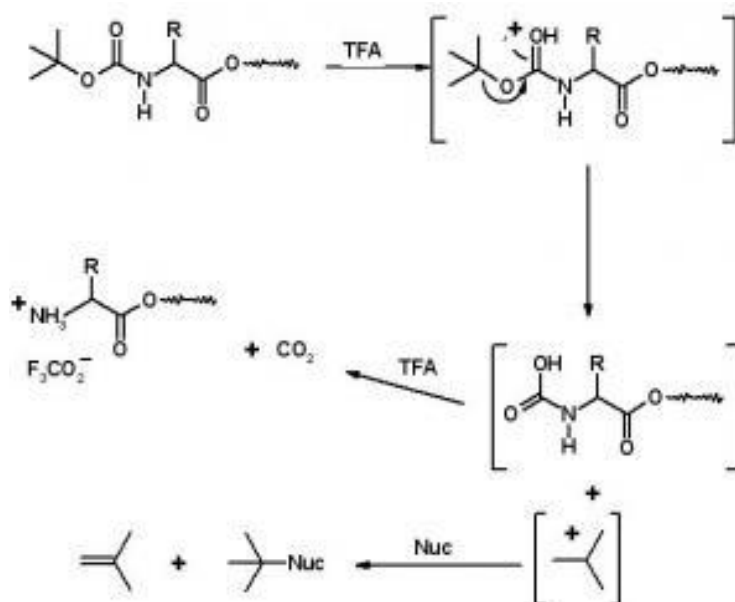
Figure2.5: Deprotection process using TFA (57)

2.1.4 – Coupling methods

In SPPS the carboxyl group of amino acids needs to be activated by reagents, for example, cyclohexylcarbodiimide (DCC) (57). Hydroxybenzotriazole (HOBt) is a common additive used in combination with carbodiimides for amide bond formation (1). However, a HOBt derivative HOAt(1-hydroxy-7-azabenzotriazole) has been shown to give better results as it is more reactive and reduces recemization (57, 63). Uronium and phosphonium salts have been described as excellent reagents. HBTU and TBTU belong to the uronium salt group, whereas PyBOP and BOP are phosphonium salts (57). However, the most popular coupling reagents are HBTU and TBTU, which are differentiated only by counterions - PF_6^- and BF_4^-, respectively. Figure 2.5 depicts the structures of different coupling reagents.
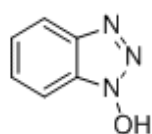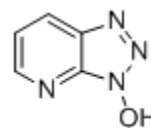
HOBt   **HOAt**
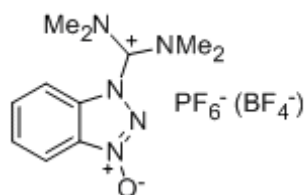
HBTU/TBTU

Figure 2.5: Hydroxybenzotriazole and derivative additive (top) and uronium salts (below) (63)

2.2 – Characterization of crude peptides

2.2.1 - Coupling High Performance Liquid Chromatography (HPLC) to a Mass Spectrometer (MS)

Chromatographic techniques, such as High Performance Liquid Chromatography (HPLC), are used to separate a mixture of compounds that are dissolved in a solution, whilst Reverse Phase (RP) HPLC is the most common method used for peptide purification (64, 65). This technique has a hydrophobic stationary phase and a hydrophilic mobile phase. In general, the column supports are composed of hydrocarbon alkane chains attached to silica (stationary phase) and the polar solvent is used in a mixture of water and an alcohol (mobile phase)(65). In this method, when a peptide solution passes through the column, a strong interaction occurs between the hydrophobic phase and apolar molecules in solvents. The attraction between stationary phase and polar molecules is low (64), while hydrophobic molecules in solution tend to form Van der Walls interactions with the stationary phase (65). Thus, the polar molecules will move through the column faster than non-polar molecules.

Mass Spectrometry (MS) is a powerful analytical tool (66, 67). Matrix-assited laser desorption ionization (MALDI) is one of the most commom ionization methods. This soft ionization technique uses a laser beam to convert biomolecules into gas phase ions that are then accelerated by an electric field and separated according to their mass-to-charge ratio (m/z) (68). The gas-phase ions are generated from a solid matrix mixture by laser, causing the vaporization of the analyte (67, 69). MALDI has the advantage of producing singly charged peptide ions, hence minimizing spectral complexity (67). When the mass is measured using the time of flight of the ions in a drift tube, the analyzer is called time of flight (ToF) (70).

ToF analysers can be operated in linear and reflectron modes (70). Figure 2.6 shows an MS apparatus where a MALDI source has been coupled with a ToF reflectron analyser.
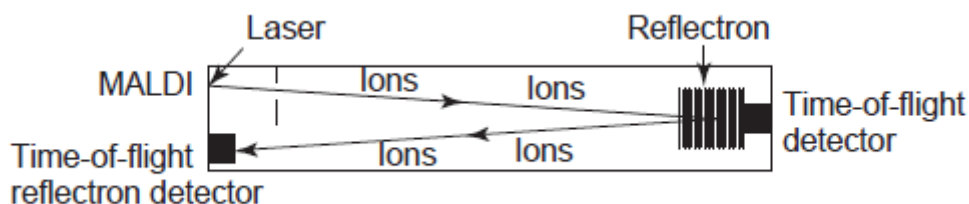
Figure 2.6: MALDi with TOF reflectron(70).

Mass spectrometers can be coupled with separation techniques such as LC. This approach can be used when previous separation of the analytes is necessary, and allows better sensitivity in the identification of the components of a mixture. (67).

2.2.2 – Circular Dichroism (CD)

Circular Dichroism (CD) spectroscopy is a technique used to determine the folding of peptides and proteins(71). This method provides important information pertaining to biomolecular conformation and is based on the different absorption of left and right circularly polarised light ($\Delta A = A_{Left} - A_{Right}$)(72). This effect occurs by chiral chromophore or placed in an asymmetric environment (71).

CD instrumentation uses a source of light with two different wavelengths. The monochromator selects the wavelength that crosses the polarizer and forms a plane-polarised and two distinct circularly polarised components. The latter pass through the modulator containing an alternating electric field, as shown in figure 2.7 (72).

This induces structural changes which make the plate transmit circularly polarised light (72, 73). The addition of A_R and A_L absorbance vectors results in radiation designed to be elliptically polarised (73). In the spectra information obtained the concentration of the peptide can be multiplied by the mean residue weight and the peptide mass can then be divided by the number of peptide bonds. This operation will then be expressed as molar ellipticity, deg $cm^2 dmol^{-1}$ (73).
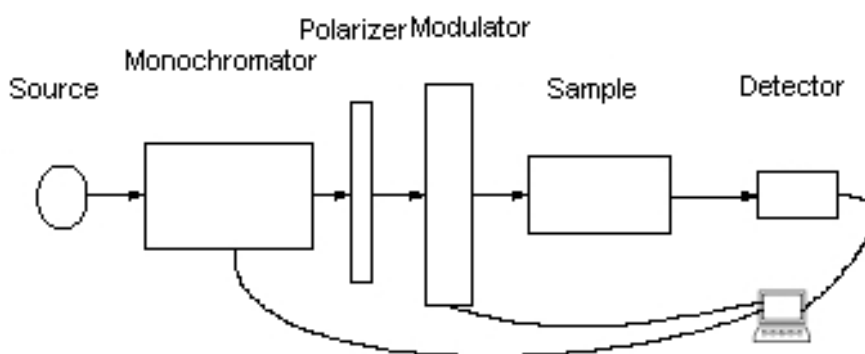
Figure 2.7: CD instrumentation

CD spectroscopy operates in far UV (260-160 nm), where it is possible to observe the contributions of the peptide bond to the change in polarised light, and also near UV (320-260 nm), where aromatic residues can be detected (71). Far UV CD is generally reported in efforts to gain an understanding of protein secondary structure (α-helix, β- sheet, β-turn and unordered content) (72). The different protein foldings put forward thus far have specific CD spectra (71). Hence, α- helix is characterized by negative bands at 222 nm and 208 nm and by a positive band at 190 nm (71). Proteins with β-sheet structure have negative bands at 216 nm and a positive band at 196 nm(71). The random coil structure is characterized by a negative band at 198 nm and a positive band at 219 nm (71). Figure 2.8 shows typical spectra for different structures.

Figure 2.8: Representative CD spectra for α-helix (blue line), β-sheet (red line) and random coil (black line) (74)

2.3 – Experimental

2.3.1 - Materials

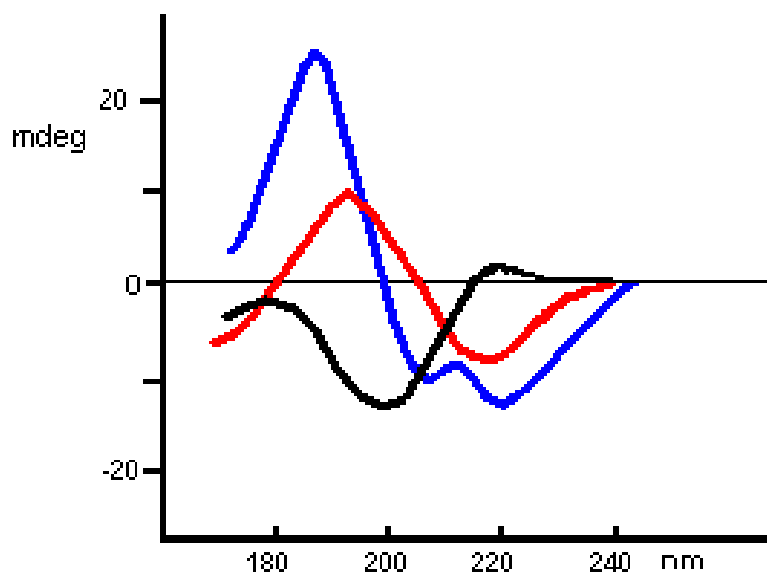The solvents for Solid Phase Peptide Synthesis were obtained from commercial suppliers. Amino acids, reagents and resins were acquired from Nova biochem and DMF for solid phase synthesis from Rathburn Chemicals.

2.3.2 – Methods

2.3.2.1 – Peptide Synthesis

Peptides were synthesised using an automated peptide synthesizer (CEM liberty) and standard solid phase Fmoc-based protocols. MBHA rink amide was used to provide peptide amides and HBTU/DIPEA deployed for use as coupling reagents. Fmoc-protected amino acids (100x 4 µmol) with HBTU/DIPEA (dilauryphosphatidyglycerol) (100 x4 µmol: 0,16g / 67µl) were dissolved in 2 ml of DMF. The resin was mixed and then washed with DMF three times.

2.3.2.2 - Fmoc and Alloc Deprotection

To achieve Fmoc deprotection the resin was treated with 20% piperidine in DMF, after which the resin was washed three times with simple DMF. This procedure was repeated after each coupling. For Alloc deprotection, the resin was treated with tetrakis$(PPh_3)_4Pd[0]$,(0,347g) dissolved in 4 ml of $CHCl_3$:AcOH:DIPEA to the ratio of 38:1:1. This being a light sensitive reaction the reactor was wrapped in aluminium foil. After 12 hours, the resin was washed three times, in the first instance with 5% sodiumdiethyldthiocarbamate in DMF (5ml), then with DIPEA in DMF (5ml), and lastly, with DMF/DCM/DMF (5).

2.3.2.3 - Cleavage of MBHA rink amide resin and removal of protection groups

All resins were cleaved using TFA/TIS/H$_2$O 95:2,5:2,5 (5 ml) for 3 hours. After cleavage, the resin was filtered and washed with this mixture and with diethyl ether to precipitate a crude product. Peptide containing cysteines were cleaved with the use of TFA/EDT/H$_2$O 95:2,5:2,5 (5 ml)

2.3.3 - RP-HPLC

Upon completion of the deprotection and cleavage processes, all the peptides were purified by analytical and semi-preparative RP-HPLC using a JASCO system and Vydac C18 analytical (5μm) and semi-preparative (5μm) columns, respectively. Running buffers A (95% H$_2$O, 5% AcCN and 0,1% TFA) and B (95%AcCN, 5% H$_2$O and 0,05%TFA) were used for10-60% B gradient over 46 min at 1 ml/min and 4.5 ml/min. The peptides were characterized by MALDI-ToF and analytical HPLC.

MS [M+H]$^+$: AC1 − m/z 2643,52 (calc), 2644,56 (found); AC3 m/z 680,98 (calc) , 682,63 (found) ; AC4 – m/z 944,32 (calc) , 944,68 (found) ; AC5 m/z 860,14 (calc) , 861,83 (found) ; AC6 – m/z 596,79 (calc) , 597,71 (found) ; AC7 – m/z 595,7 (calc) , 598,47 (found) ; AC8 – m/z 860,14 (calc) , 860,78 (found) ; AC9 m/z 944,33 (calc) , 945,93 (found)

2.3.4 - Circular Dichroism

Circular Dichroism spectroscopy was performed on a Chirascan plus. All measurements were taken in ellipticities(mdeg) and then converted into molar ellipticities (deg cm^2 dmol res $^{-1}$) and normalized for the number of peptide bonds required. The stock solutions were prepared in water except those for the peptides with

cysteines, which were dissolved in aqueous 1mM TCEP. All aqueous solutions of the samples were prepared in filtered 10mM MOPS at pH 7.4.

2.3.5 - Transmission Electron Microscopy

TEM was performed using a JEOL JEM 1200EX MKI microscope at the accelerating voltage of 100 kV and the images acquired with a fitted camera (MegaViewII). The sample (100 µM peptide concentrations) was prepared in 200 ml of 10 mM MOPS at pH 7.4 and incubated overnight at 20° C.

2.3.6 - Antibacterial activity

Minimum inhibitory concentrations (MIC) were defined as the lowest peptide concentration in which no visible growth of a microorganism was observed after 24 hours incubation at 37 C. MIC were determined by microdilution on *Pseudomonas aeruginosa*, *Escherichia coli* and *Staphylococus aeruginosa*. All tests were performed in duplicate.

Chapter 3 - Self-Assembly of peptide-amphiphile

3.1-Introduction

Biomolecular systems have been developed as biomaterials, which are generally designed from biological structural units such as peptides and proteins (5). The self-assembly process is a powerful tool for the synthesis of these novel biomaterials, which are highly promising for medical research (5). Different classes of hybrid materials have been explored over the years. Peptide amphiphiles (PAs) are a particularly interesting and attractive class of self-assembling systems due to their potential for use in tissue engineering (58). The structures are characterized by a peptide sequence linked to an alkyl tail via the N-terminus. PAs have the capacity to organize into micelle-like cylindrical nanofibres in an aqueous solution owing to the intermolecular hydrogen bonding that is intrinsic to them (40). In micelle formation, alkyl chains form a hydrophobic core while the peptide segments are solvent-exposed. The formation of nanofibre structures results in a high density of peptide epitopes and allows mineralization to occur.

PAs are biocompatible and biodegradable as they are composed of natural amino acids and lipids. The design principles for PAs have been extensively explored using a wide range of molecules with specific amino acid sequences (51).

The α-helical structure is present in many proteins with important biological functions, such as antibiotics, transcription factors, muscle protein tropomyosin, tumour suppressor factors and cytoskeleton proteins. Helical domains often assemble into helical bundles or coiled coils. These are attracting a great deal of interest within the scientific community due to their potential and promise in the design of new peptide-based materials. Coiled coils and helices are characterized by heptad repeats of hydrophobic (H) and polar (P) amino acids in their sequences, PHPPHPP.

Different antimicrobial peptides, many of which adopt helical conformations, have thus far been described. These peptides may be classified into several different groups according to their structure, origin and activity (75). Most of these peptides are cationic and can adopt amphipathic structures formed by the clustering of

hydrophobic and cationic residues (76). The mechanism of their biological activity is not yet fully understood, but peptides are predicted to bind negatively charged surfaces of Gram-negative and Gram-positive bacteria (75).

In this chapter a helical design and a set of PAs with short peptide (3-5 amino acids) sequences attached to a hydrophobic domain are described. These peptides were characterized using molecular biophysics and biological testing.

3.2-Results and discussion

3.2.1 – α- helix – amphiphile structure

AC1 peptide is built of two amino-acids types: hydrophobic (H) and polar (P). The sequence is linked to an aliphatic hydrophobic tail to promote micelle-like oligomerisaton (figure 3.1a). The hydrophobic residues in the sequence are alternating Ile and Leu residues, whilst cationic residues consist of Lys and Gln and polar residues of Ala.

This construct was achieved by means of a flexible linker of two β-alanine residues inserted between the amino-acid sequence and the hydrophobic tail, lauric acid (C_{12}), to provide a nonspecific micelle formation. In water amphiphile peptide self-assembles to create cylindrical micelles with alkyl tails occupying their centre (figure3.1b).

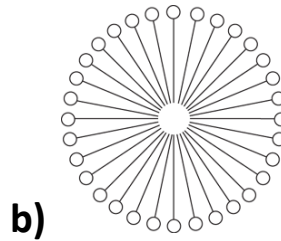## a) C$_{12}$- $_\beta$A-$_\beta$A-KIAKLKAKIQKLKQKIAKLK

b)

Figure3.1: Lipoprotein design a) Peptide sequence used in the study b) schematic of micelle structure

Circular dichroism (CD) spectroscopy with three different concentrations (50 μM, 100 μM and 200 μM) at pH7 showed predominantly random coil conformations with some elements of a helical structure (figure 3.2). Figure 3.3 illustrates the CD spectra thermal denaturation (melting up to 90 C) for peptide AC1. Both spectra revealed negative peaks at 208 and 222 nm and a positive peak at 218 nm.

Transmission Electron Microscopy (TEM) revealed fibrillar structures (figure 3.4). The fibres were found to have diameters of approximately 10-20 nm which at elevated temperatures increased to approximately 0,8μm diameters. This is consistent with the fact that assembly is driven primarily by the hydrophobic effect, and the peptide does not fold in a solution and in the absence of negatively charged bacterial membranes.
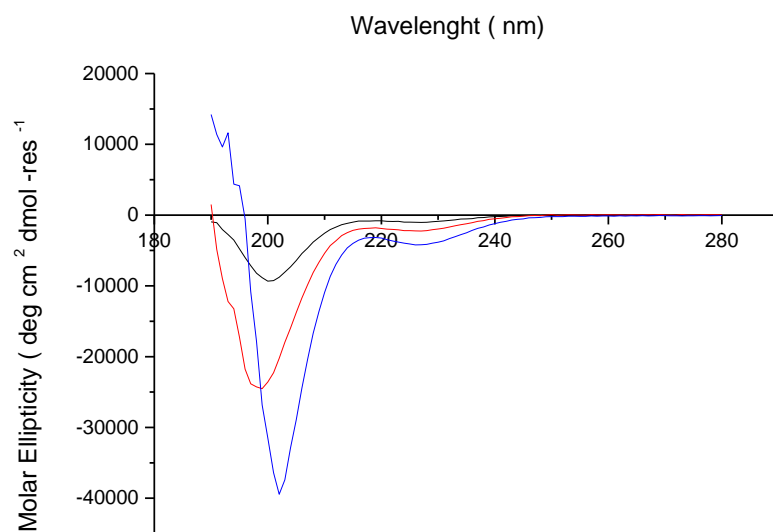
Wavelenght (nm)

Figure 3.2: CD spectra at 20° C for AC1 at 50 μM (black line), 100μM (red line), 200 μ (blue line) in 10 mM MOPS.
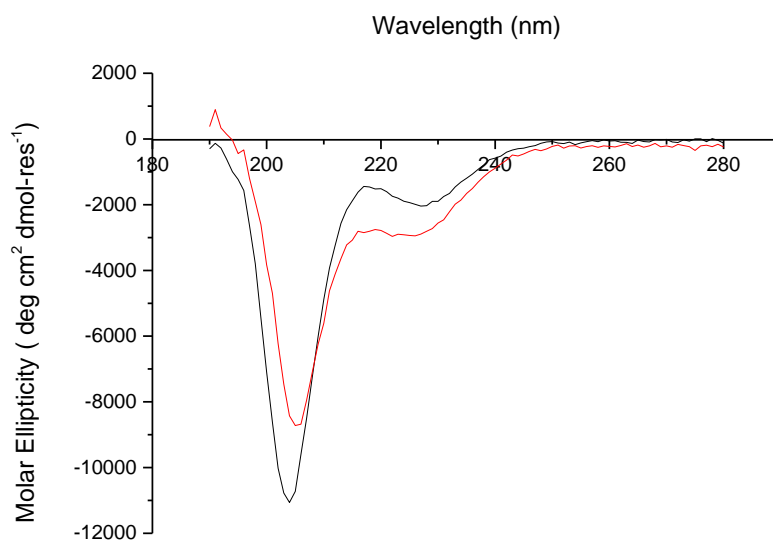

Wavelength (nm)

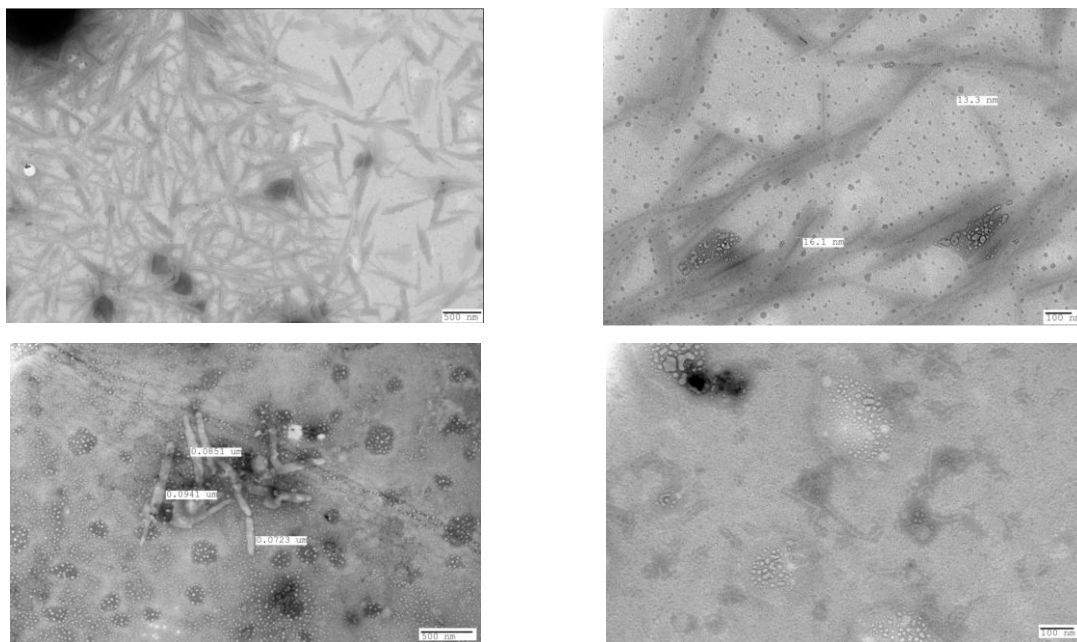**Figure 3.3: CD spectra for peptide AC1 at 10º C (black line) and at 90º C (red line) in 10 mM MOPS.**

Figure 3.4: Negatively stained transmission electron micrographs of peptide AC1. Assembly conditions in 10 μM MOPS at pH 7.4, left overnight at 20° C (top) at melting (below)

To reveal the antimicrobial properties of this peptide, a series of biological tests were performed. Peptide AC1 was tested against Gram-negative (*Escherichia coli* and *Pseudomonas aeruginosa*) and Gram-positive (*Staphylococcus aureus*) bacteria using microdilution assays. Figures 3.5, 3.6 and 3.7 illustrate the results of antimicrobial activity for the three bacteria tested.
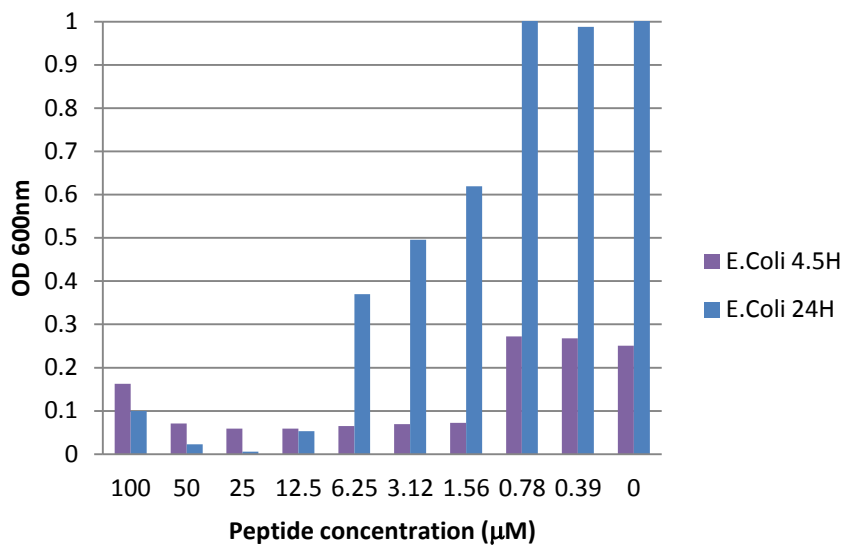
Figure 3.5: Antimicrobial activity for *Escherichia coli* at 4.5 hours and 24 hours. Each value was done in duplicate.
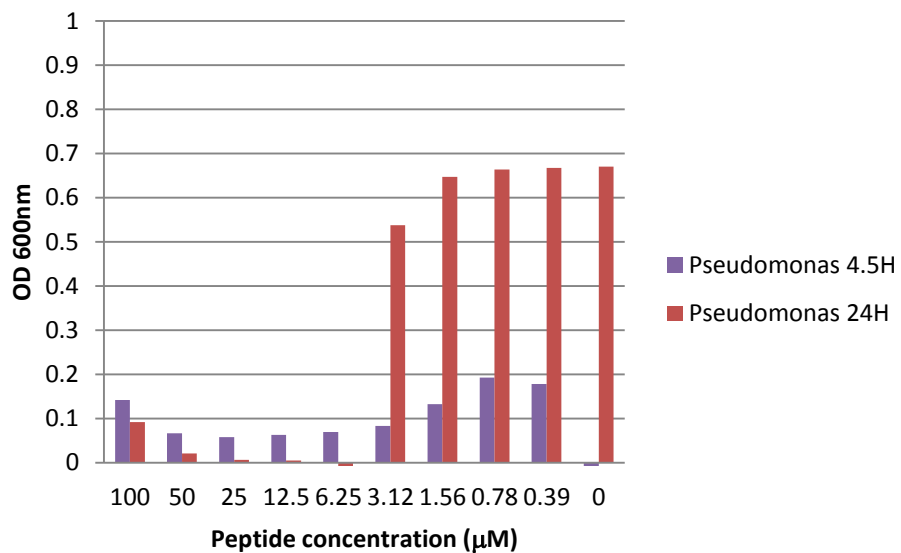

Figure 3.6: Antimicrobial activity for *Pseudomonas aeruginosa* at 4.5 hours and 24 hours. Each value was done in duplicate.
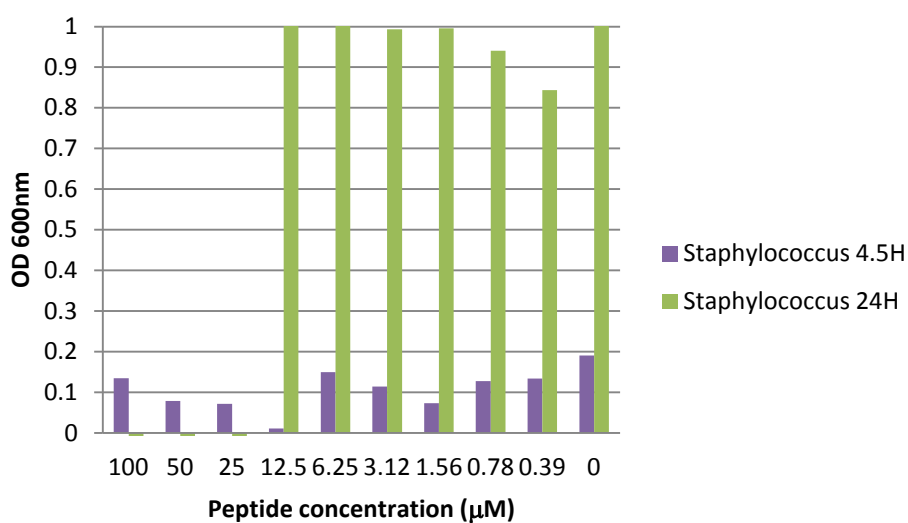
Figure3.7: Antimicrobial activity for *Staphylococcus aureus* at 4.5 hours and 24 hours. Each value was done in duplicate.

The peptide was noticeably active against all three bacteria. The Minimal Inhibitory Concentration (MIC) for *Escherichia coli*, *Pseudomonas aeruginosa* and *Staphylococcus aureus* was 12.5 µM, 6.25 µM and 25 µM, respectively. These results suggest that the peptide may have preference for targeting Gram-negative bacteria.

Upon comparison of eukaryotic and microbial membranes, the microbial membranes are found to be anionic. Therefore, the antimicrobial activity confirms the designed selectivity to permeabilize anionic membranes.

3.2.3 –Peptide-Amphiphile Structure

In this work eight different PAs were designed and synthesized. The design was of an amphiphilic motif comprising a hydrophobic aliphatic tail, stearic acid (C_{18}), and a hydrophilic peptide sequence. The peptides were designed to possess weak antimicrobial properties that may be enhanced by the self-assembly process; that is, through the contact of assembled structures with bacterial cells. The first series of peptide-amphiphile (AC 2-5) is shown in figure 3.8. In AC4 and AC5, two cysteine residues provide intermolecular thiol cross-linking between peptides to promote oligomerization.

AC2

$C_{18}QLR$

AC3

$C_{18}Q(L)R$

AC4

C_{18}**CGCQLR**

AC5

C_{18}**CGCQ(L)R**
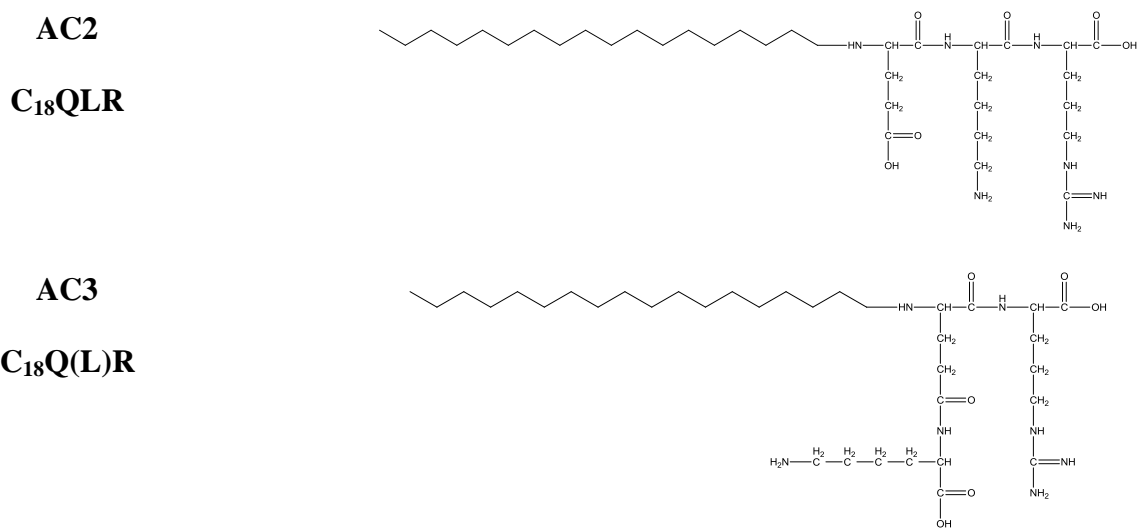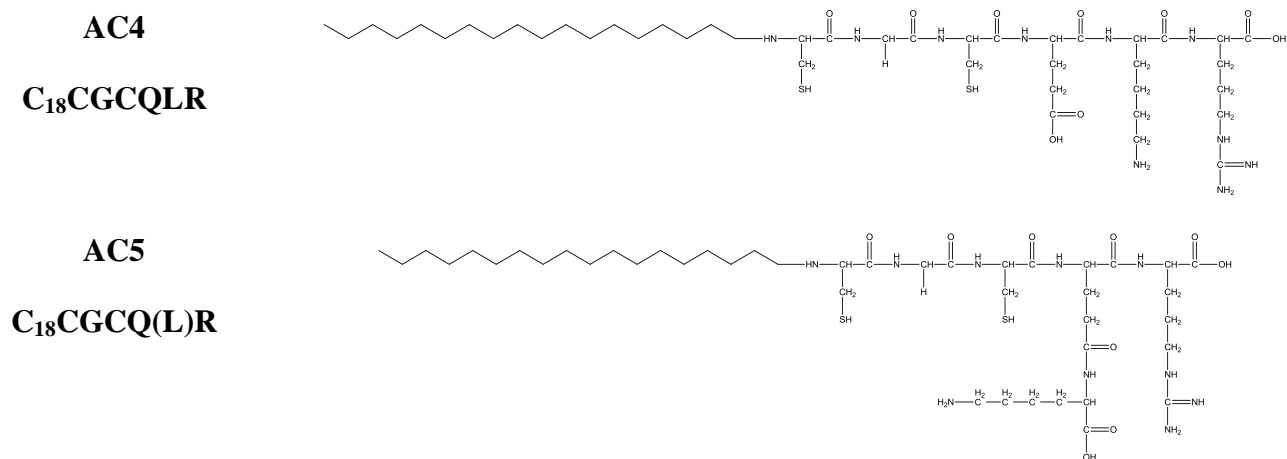
Figure 3.8: Peptide –amphiphile types used in the study

AC2 posed solubilisation difficulties, which hindered its purification and biophysical characterisation. CD spectroscopy revealed signals characteristic of β-sheet conformations for AC4 peptide (figure 3.10). The spectra have a negative peak between 218 and 220 nm and a positive peak at 200 nm. However, the spectra for AC3 and AC5 were less resolved suggesting weak β-sheet or random coil conformations (Figure 3.9 and Figure 3.11).

Figure 3.9: CD spectra at 20ºC for peptide AC3 at 50 µM (black line), 100µM (red line), 200 µ (blue line).
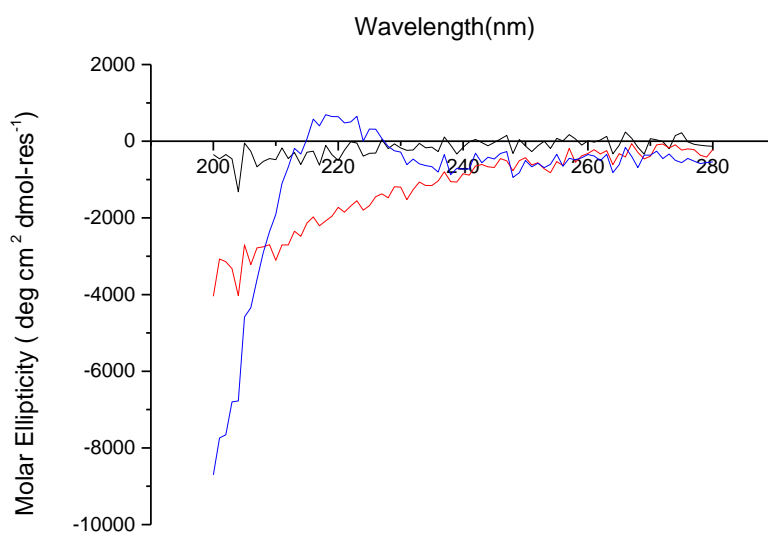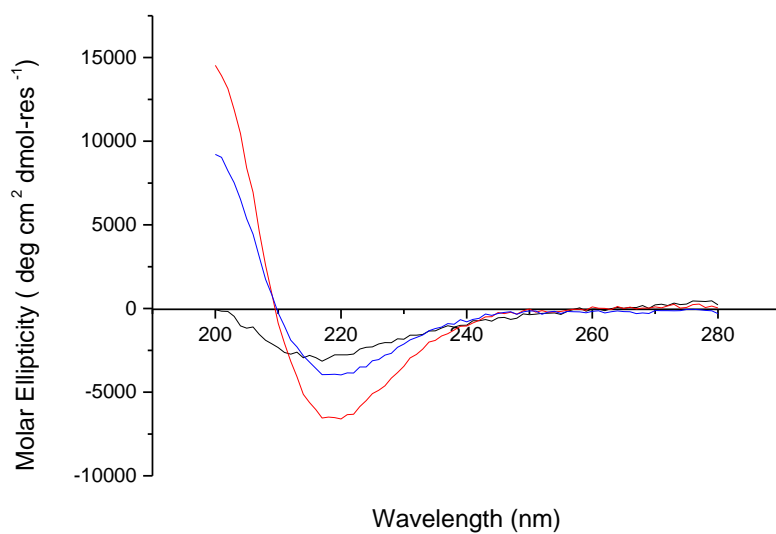

Figure 3.10: CD spectra at 20ºC for peptide AC4 at 50 µM (black line), 100µM (red line), 200 µM (blue line).
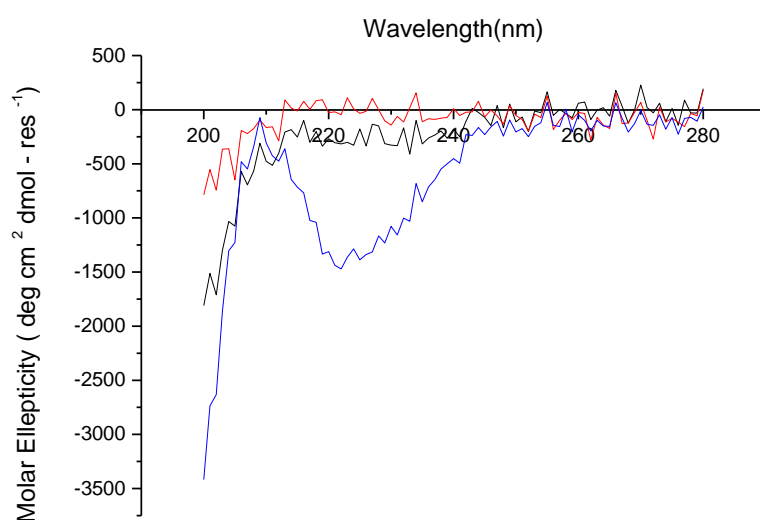
Figure 3.11: CD spectra at 20ºC for peptide AC5 at 50 µM (black line), 100µM (red line), 200 µM (blue line).

The formation of supramolecular structures was assessed by Transmission Electron Microscopy (TEM). In all cases, the PAs assembled into nanofibres but with different diameters and structures. Figure 3.12 and 3.13 shows the nanofibres of all peptide-amphiphile of this series. AC4 formed nanofibres with the diameters of approximately 5-10 nm and AC3 and AC5 assembled into extensive fibrillar networks of different morphologies.
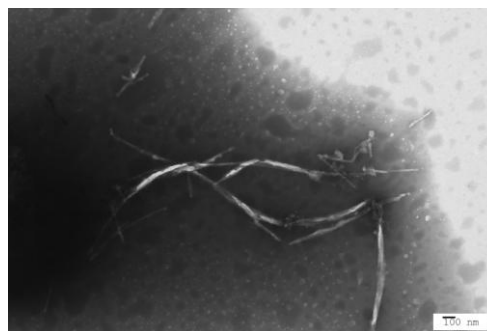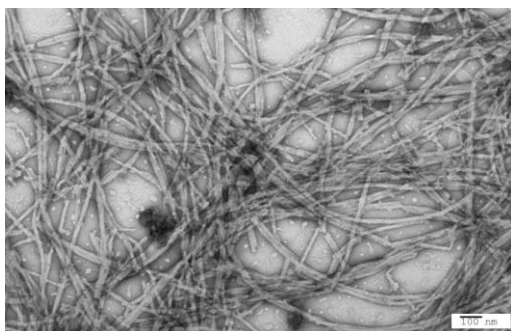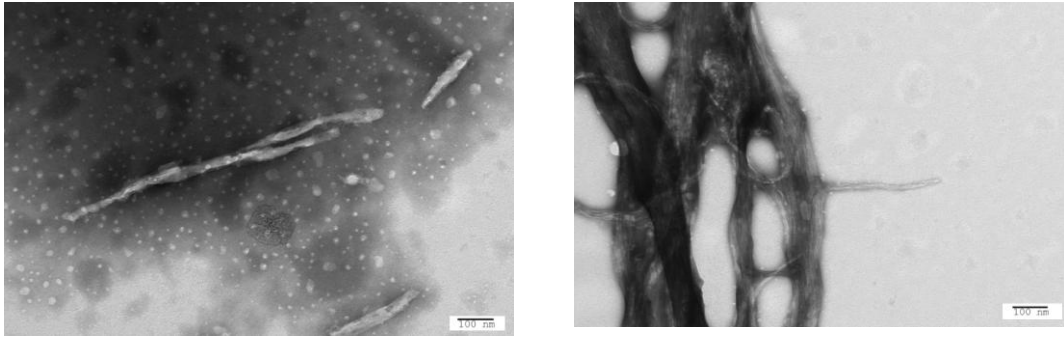
Figure 3.12: Negatively stained transmission electron micrographs of peptide AC3. Assembly conditions in 10 μM MOPS at pH 7.4, left overnight 20° C.
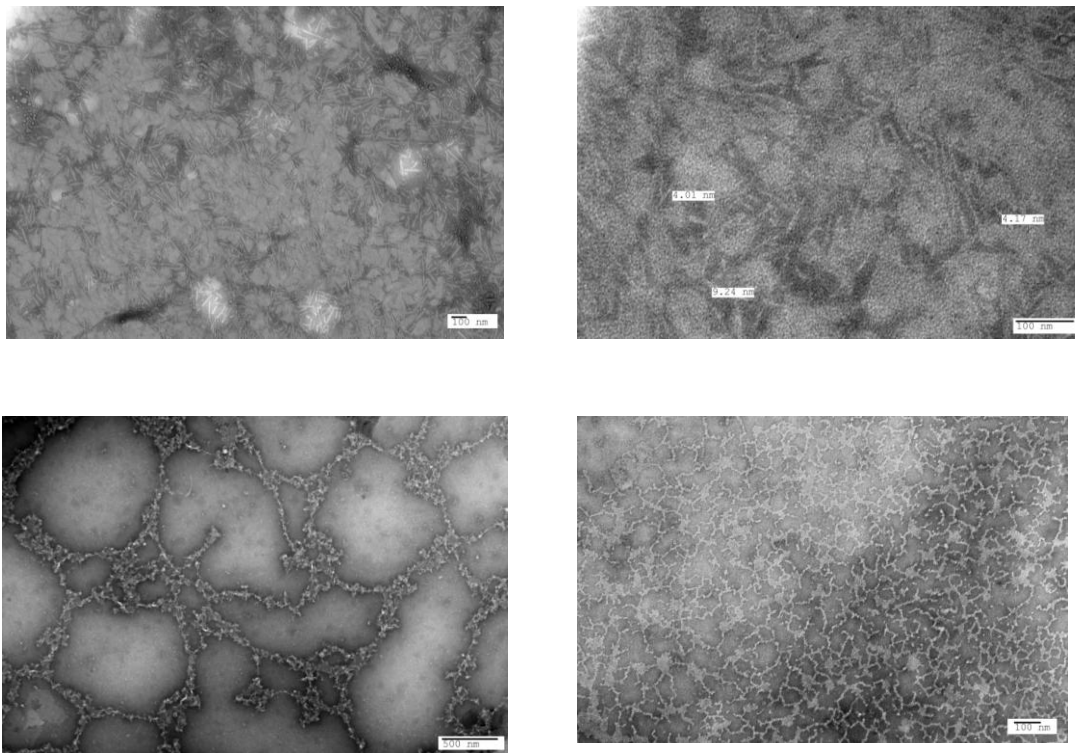
Figure 3.13: Negatively stained transmission electron micrographs of peptide AC4 (top) and peptide AC5 (below). Assembly conditions in 10 μM MOPS at pH 7.4, left overnight at 20° C.

All peptides were also tested against Gram-negative (*Escherichia coli* and *Pseudomonas aeruginosa*) and Gram-positive (*Staphylococcus aureus*) bacteria. As expected, weak antimicrobial activities were observed for all peptides using standard microdilution assays (table 1).

Table 1: Minimal Inhibitory Concentration in µM

	AC3	**AC4**	**AC5**
Escherichia coli	>100	>100	>100
Pseudomonas aeruginosa	>100	>100	>100
Staphylococcus aureus	>100	>100	>100

The second series of PAs (AC6-AC9) was prepared to determine the effect of the length of the hydrophobic domain in fibre formation. Thus, the difference between this series and the first series is the length of the hydrophobic tail used. All peptides were linked at their N-termini with lauric (C_{12}) acid to enable micelle formation (figure 3.14).

AC6

C₁₂QLR

AC7

C₁₂Q(L)R

AC8

C₁₂CGCQLR

AC9

C₁₂CGCQ(L)R
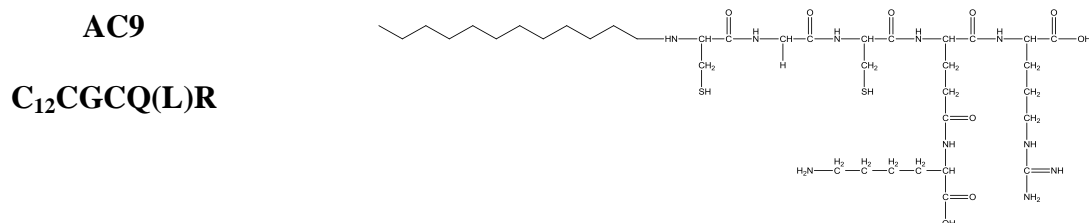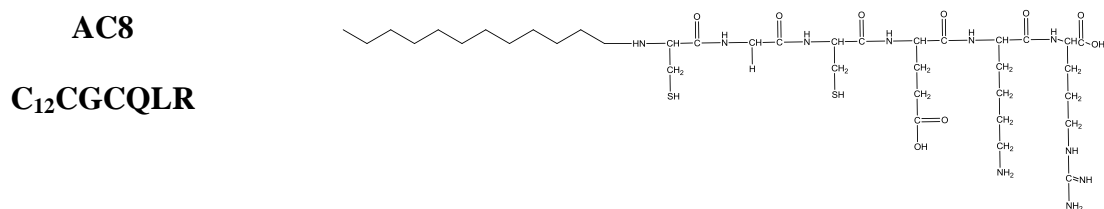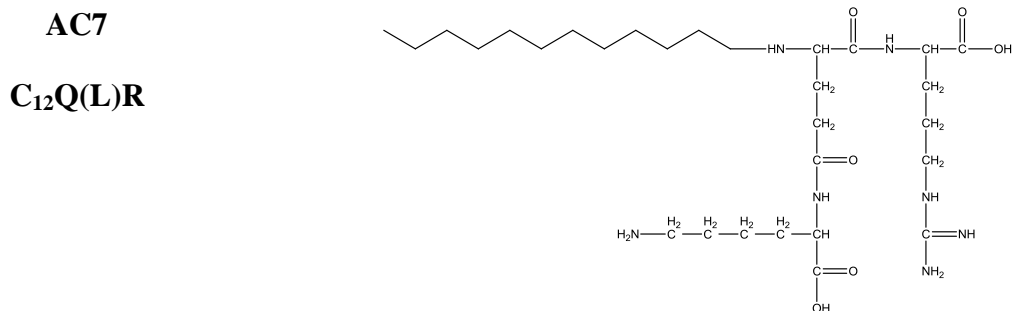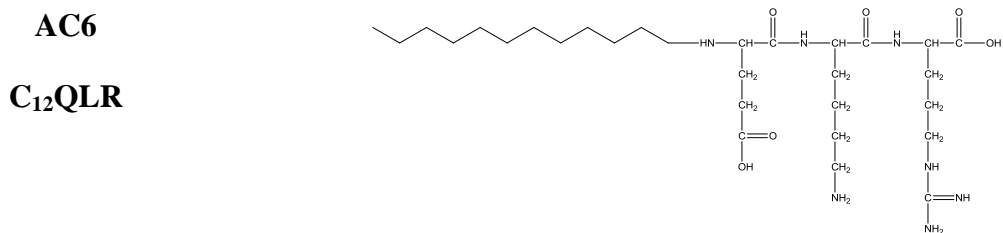
Figure 3.14: PA types used in the study.

The secondary structure in aqueous solution was determinate by CD spectroscopy. In all cases, a main negative peak at 200 nm as for AC6, AC7, AC8 and AC9 was observed suggesting a predominant random coil conformation (figures 3.15-3.18).

TEM revealed random aggregates for all amphiphiles, which in some cases resembled fibrillar assemblies of very low densities (figures 3.19 and 3.20). This is consistent with the CD data and suggests weakened self-assembly properties of the first series as a result of shortened length of the aliphatic chain.
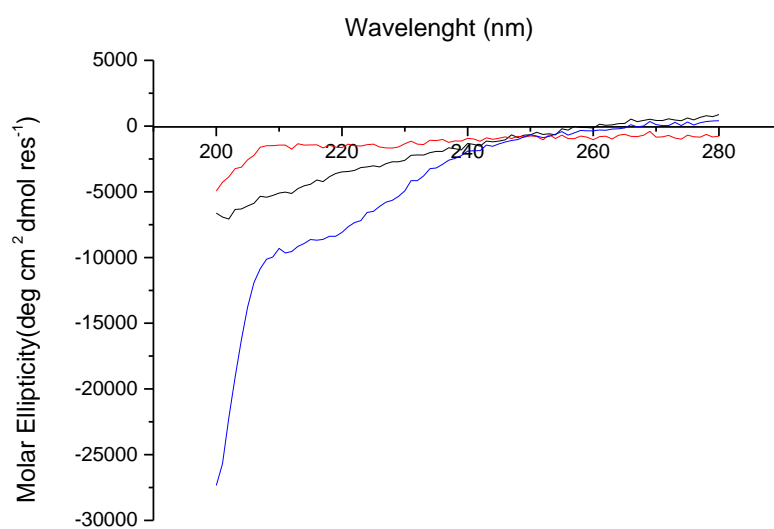
Figure 3.15: CD spectra at 20°C for AC6 at 50 µM (black line), 100µM (red line), 200 µM (blue line).
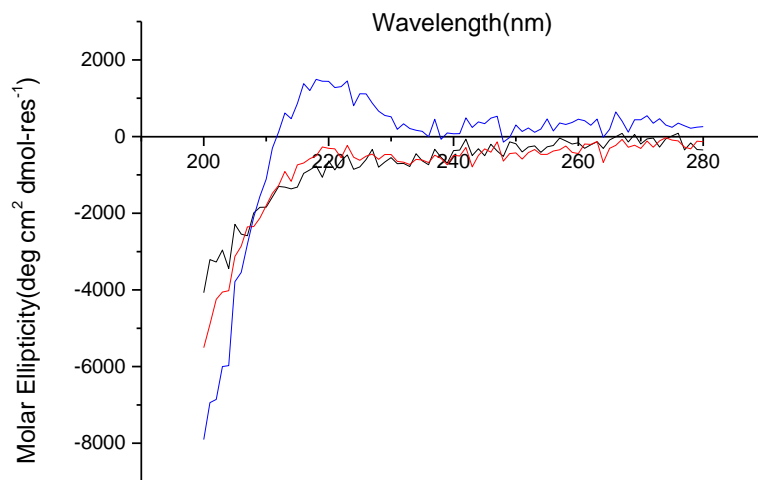
Figure 3.16: CD spectra at 20°C for peptide AC7 at 50 µM (black line), 100µM (red line), 200 µM (blue line).

Figure 3.17: CD spectra at 20°C for peptide AC8 at 50 µM (black line), 100µM (red line), 200 µM (blue line).
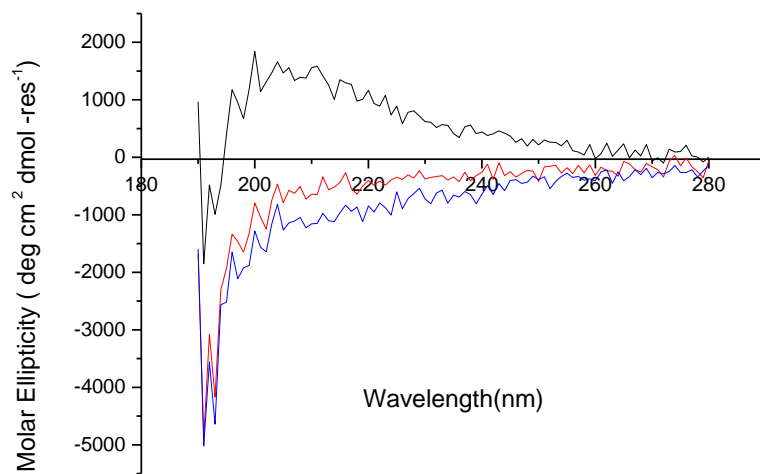
Figure 3.18: CD spectra at 20° C for peptide AC9 at 50 µM (black line), 100µM (red line), 200 µM (blue line).
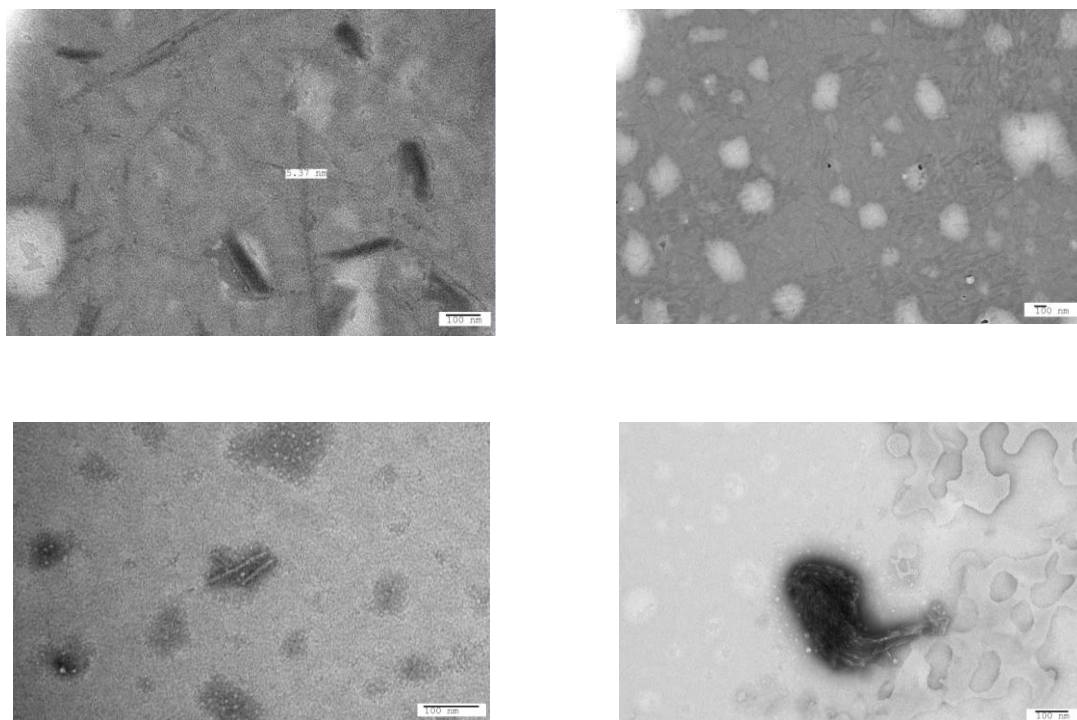
Figure 3.19: Negatively stained transmission electron micrographs of peptide AC6 (top) and peptide AC7 (below). Assembly conditions in 10 µM MOPS at pH 7.4, left overnight at 20° C.
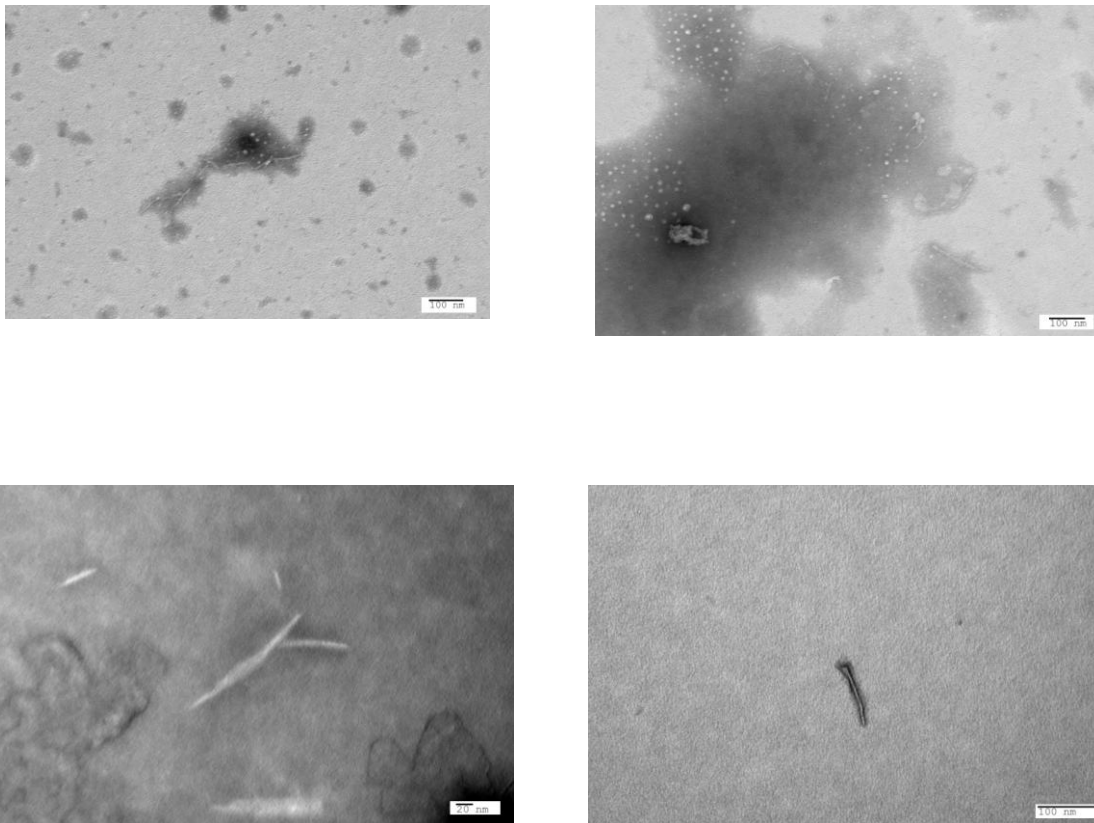
Figure 3.20: Negatively stained transmission electron micrographs of peptide AC8 (top) and peptide AC 9 (below). Assembly conditions in 10 μM MOPS at pH 7.4, left overnight at 20° C.

Antimicrobial tests revealed inconsistent results to judge the difference in behaviour between the peptides. None of the compounds except AC8 demonstrated visible activity against the bacterial cells using microdilution assays (Table 2), suggesting that all peptides possess weak antimicrobial activities for Minimal Inhibitory Concentrations (MICs) of ≤ 100 μM .

Table 2: Minimal Inhibitory Concentration in µM

	AC6	AC7	AC8	AC9
Escherichia coli	>100	>100	100	>100
Pseudomonas aeruginosa	>100	>100	100	>100
Staphylococcus aureus	>100	>100	100	>100

General conclusion and future work

Several examples of designer materials were described in this work. Three different series of peptide amphiphiles were generated. Specifically, AC1 was strongly antibacterial, adopted partially helical conformations and assembled into nanoscale fibrillar structures. It is strongly antimicrobial and its activity appears to be more efficient against Gram-negative than against Gram-positive bacteria. A generic approach based on peptide self-assembly to generate nanoscale fibrillar biomaterials was also described herein. Two different series of shorter designed lipopeptides were predominant in random coil conformations and some formed beta-sheet structures as judged by circular dichroism. The approach offers straight forward lipopeptide self-assembly templates leading to different fibrillar morphologies. A range of morphologies from elongated micron-sized fibrils to complex fibre networks were observed. Assembly appeared to be consistent with folding tendencies: more pronounced fibres were observed for more structured PAs. Biological properties of the building blocks (AC2-9) regarding potential antimicrobial activities were assessed. Individually, none of the blocks was strongly antimicrobial, which is consistent with the fact that antimicrobial properties have to be enhanced by fibrillar assembly and executed through direct contacts between fibre surfaces and the bacterial cell. This is currently being tested and constitutes future studies. The resulting fibrillar materials may be readily modified with different amino acids to provide different biological properties, such as cell adhesion support and biomineralization.

This work demonstrates the feasibility of PA folding for self-assembled fibrillar materials that may find use in the design of novel biomaterials in applications for tissue engineering and biomedicine.

References

1. O'Brien FJ. Biomaterials & scaffolds for tissue engineering. Materials Today. 2011;14(3):88-95.

2. Gromiha MM. Chapter 1 - Proteins. Protein Bioinformatics. Singapore: Academic Press; 2010. p. 1-27.

3. Shu JY, Xu T. 7.08 - Peptide–Polymer Conjugates Toward Functional Hybrid Biomaterials. In: Editors-in-Chief: Krzysztof M, Martin M, editors. Polymer Science: A Comprehensive Reference. Amsterdam: Elsevier; 2012. p. 141-58.

4. Bose S, Bandyopadhyay A. Chapter 1 - Introduction to Biomaterials. In: Amit B, Susmita B, editors. Characterization of Biomaterials. Oxford: Academic Press; 2013. p. 1-9

5. Reid B, Elisseeff J. 5.516 - Biomaterials in Cartilage Tissue Engineering. In: Editor-in-Chief: Paul D, editor. Comprehensive Biomaterials. Oxford: Elsevier; 2011. p. 213-20.

6. Zhang S. Fabrication of novel biomaterials through molecular self-assembly. Nature biotechnology. 2003;21(10):1171-8.

7. Hubbell JA. Biomaterials in Tissue Engineering. Nature Publishing group.

8. Zhao X, Pan F, Lu JR. Recent development of peptide self-assembly. Progress in Natural Science. 2008;18(6):653-60.

9. Cui F-Z, Li Y, Ge J. Self-assembly of mineralized collagen composites. Materials Science and Engineering: R: Reports. 2007;57(1–6):1-27.

10. Kyle S, Aggeli A, Ingham E, McPherson MJ. Recombinant self-assembling peptides as biomaterials for tissue engineering. Biomaterials. 2010;31(36):9395-405.

11.   Amdursky N, Molotskii M, Gazit E, Rosenman G. Elementary Building Blocks of Self-Assembled Peptide Nanotubes. Journal of the American Chemical Society. 2010 2010/11/10;132(44):15632-6.

12.   Kyle S, Aggeli A, Ingham E, McPherson MJ. Production of self-assembling biomaterials for tissue engineering. Trends in biotechnology. 2009;27(7):423-33.

13.   Wang X-m, Qiao L, Horii A. Screening of functionalized self-assembling peptide nanofiber scaffolds with angiogenic activity for endothelial cell growth. Progress in Natural Science: Materials International. 2011;21(2):111-6.

14.   Lamm MS, Rajagopal K, Schneider JP, Pochan DJ. Laminated Morphology of Nontwisting β-Sheet Fibrils Constructed via Peptide Self-Assembly. Journal of the American Chemical Society. 2005 2005/11/01;127(47):16692-700.

15.   Glembo TJ, Ozkan SB. Union of Geometric Constraint-Based Simulations with Molecular Dynamics for Protein Structure Prediction. Biophysical journal. 2010;98(6):1046-54.

16.   Waldispühl J, Steyaert J-M. Modeling and predicting all- transmembrane proteins including helix–helix pairing. Theoretical Computer Science. 2005;335(1):67-92.

17.   Flower DR. β-Sheet topology A new system of nomenclature. FEBS Letters. 1994;344(2–3):247-50.

18.   Parry DAD, Fraser RDB, Squire JM. Fifty years of coiled-coils and α-helical bundles: A close relationship between sequence and structure. Journal of Structural Biology. 2008;163(3):258-69.

19.   Levin S, Nowick JS. A New Artificial β-Sheet That Dimerizes through Parallel β-Sheet Interactions. Organic Letters. 2009 2009/02/19;11(4):1003-6.

20.   Koga T, Matsuoka M, Higashi N. Structural Control of Self-Assembled Nanofibers by Artificial β-Sheet Peptides Composed of d- or l-Isomer. Journal of the American Chemical Society. 2005 2005/12/01;127(50):17596-7.

21.   Shifman JM. Intricacies of ² Sheet Protein Design. Structure (London, England : 1993). 2008;16(12):1751-2.

22.   Makabe K, Koide S. The Promiscuity of β-Strand Pairing Allows for Rational Design of β-Sheet Face Inversion. Journal of the American Chemical Society. 2008 2008/11/05;130(44):14370-1.

23.   Leon L, Logrippo P, Tu R. Self-Assembly of Rationally Designed Peptides under Two-Dimensional Confinement. Biophysical journal. 2010;99(9):2888-95.

24.   Cisneros DA, Hung C, Franz CM, Muller DJ. Observing growth steps of collagen self-assembly by time-lapse high-resolution atomic force microscopy. Journal of Structural Biology. 2006;154(3):232-45.

25.   Cen L, Liu W, Cui L, Zhang W, Cao Y. Collagen tissue engineering: development of novel biomaterials and applications. Pediatric research. 2008;63(5):492-6.

26.   Wang AY, Mo X, Chen CS, Yu SM. Facile Modification of Collagen Directed by Collagen Mimetic Peptides. Journal of the American Chemical Society. 2005 2005/03/01;127(12):4130-1.

27.   Gelse K, Pöschl E, Aigner T. Collagens—structure, function, and biosynthesis. Advanced Drug Delivery Reviews. 2003;55(12):1531-46.

28.   Bella J. A new method for describing the helical conformation of collagen: Dependence of the triple helical twist on amino acid sequence. Journal of Structural Biology. 2010;170(2):377-91.

29.   Orgel JPRO, Miller A, Irving TC, Fischetti RF, Hammersley AP, Wess TJ. The In Situ Supermolecular Structure of Type I Collagen. Structure. 2001;9(11):1061-9.

30.   Steplewski A, Ito H, Rucker E, Brittingham RJ, Alabyeva T, Gandhi M, et al. Position of single amino acid substitutions in the collagen triple helix determines their effect on structure of collagen fibrils. Journal of Structural Biology. 2004;148(3):326-37.

31.   Fallas JA, Lee MA, Jalan AA, Hartgerink JD. Rational Design of Single-Composition ABC Collagen Heterotrimers. Journal of the American Chemical Society. 2011 2012/01/25;134(3):1430-3.

32.   Rele S, Song Y, Apkarian RP, Qu Z, Conticello VP, Chaikof EL. D-Periodic Collagen-Mimetic Microfibers. Journal of the American Chemical Society. 2007 2007/11/01;129(47):14780-7.

33.   Arndt KM, Pelletier JN, Müller KM, Plückthun A, Alber T. Comparison of In Vivo Selection and Rational Design of Heterodimeric Coiled Coils. Structure. 2002;10(9):1235-48.

34.   Potekhin SA, Melnik TN, Popov V, Lanina NF, Vazina AA, Rigler P, et al. De novo design of fibrils made of short α-helical coiled coil peptides. Chemistry & Biology. 2001;8(11):1025-32.

35.   Moutevelis E, Woolfson DN. A Periodic Table of Coiled-Coil Protein Structures. Journal of Molecular Biology. 2009;385(3):726-32.

36.   Bromley E, Sessions R, Thomson A, Woolfson D. Designed α-Helical Tectons for Constructing Multicomponent Synthetic Biological Systems. Journal of the American Chemical Society. 2009;131(3):928-30.

37.   Schnarr NA, Kennan AJ. Strand Orientation by Steric Matching: A Designed Antiparallel Coiled-Coil Trimer. Journal of the American Chemical Society. 2004 2004/11/01;126(44):14447-51.

38.   Oakley MG, Hollenbeck JJ. The design of antiparallel coiled coils. Current Opinion in Structural Biology. 2001;11(4):450-7.

39.   Papapostolou D, Smith AM, Atkins EDT, Oliver SJ, Ryadnov MG, Serpell LC, et al. Engineering nanoscale order into a designed protein fiber. Proceedings of the National Academy of Sciences. 2007;104(26):10853-8.

40.   Fry HC, Garcia JM, Medina MJ, Ricoy UM, Gosztola DJ, Nikiforov MP, et al. Self-Assembly of Highly Ordered Peptide Amphiphile Metalloporphyrin Arrays. Journal of the American Chemical Society. 2012 2012/09/12;134(36):14646-9.

41.   Ryadnov MG, Woolfson DN. Self-Assembled Templates for Polypeptide Synthesis. Journal of the American Chemical Society. 2007 2007/11/01;129(45):14074-81.

42.   White GE, Erickson HP. Sequence divergence of coiled coils—structural rods, myosin filament packing, and the extraordinary conservation of cohesins. Journal of Structural Biology. 2006;154(2):111-21.

43.   Stupp SI. Self-Assembly and Biomaterials. Nano Letters. 2010 2010/12/08;10(12):4783-6.

44.   Dong H, Paramonov SE, Hartgerink JD. Self-Assembly of α-Helical Coiled Coil Nanofibers. Journal of the American Chemical Society. 2008 2008/10/15;130(41):13691-5.

45.   Pandya MJ, Spooner GM, Sunde M, Thorpe JR, Rodger A, Woolfson DN. Sticky-End Assembly of a Designed Peptide Fiber Provides Insight into Protein Fibrillogenesis†. Biochemistry. 2000 2000/08/01;39(30):8728-34.

46.	O'Shea EK, Lumb KJ, Kim PS. Peptide Velcro : Design of a heterodimeric coiled coil. Current biology : CB. 1993;3(10):658-67.

47.	Ryadnov MG, Woolfson DN. Engineering the morphology of a self-assembling protein fibre. Nature materials. 2003;2(5):329-32.

48.	Lee O-S, Cho V, Schatz GC. Modeling the Self-Assembly of Peptide Amphiphiles into Fibers Using Coarse-Grained Molecular Dynamics. Nano Letters. 2012 2012/09/12;12(9):4907-13.

49.	Rexeisen EL, Fan W, Pangburn TO, Taribagil RR, Bates FS, Lodge TP, et al. Self-Assembly of Fibronectin Mimetic Peptide-Amphiphile Nanofibers. Langmuir. 2009 2010/02/02;26(3):1953-9.

50.	Deng M, Yu D, Hou Y, Wang Y. Self-assembly of Peptide−Amphiphile C12−Aβ(11−17) into Nanofibrils. The Journal of Physical Chemistry B. 2009 2009/06/25;113(25):8539-44.

51.	Hartgerink JD, Beniash E, Stupp SI. Self-assembly and mineralization of peptide-amphiphile nanofibers. Science (New York, NY). 2001;294(5547):1684-8.

52.	Paramonov SE, Jun H-W, Hartgerink JD. Self-Assembly of Peptide−Amphiphile Nanofibers: The Roles of Hydrogen Bonding and Amphiphilic Packing. Journal of the American Chemical Society. 2006 2006/06/01;128(22):7291-8.

53.	Borgia JA, Fields GB. Chemical synthesis of proteins. Trends in biotechnology. 2000;18(6):243-51.

54.	Ganesan A. Solid-Phase Synthesis in theTwenty-First Century. Bentham Science Publishers Ldt. [Review]. 2006.

55.	Babu S. One Hundred Years of Peptide Chemistry 2001.

56.   Kent SBH. Chemical Synthesis pf peptides and proteins. Annual Reviews. [Review].

57.   Bodanszky M. Principles of Peptide Synthesis. Berlin Heidelberg New York Tokyo: Springer-Verlag

58.   Fernando Albericio FGM. Solid supports for the synthesis of peptides. Chemistry Today.26.

59.   Dean T. A Practical Introduction to Solid Phase Chemistry1998.

60.   Gordon K, Balasubramanian S. Solid phase synthesis – designer linkers for combinatorial chemistry: a review. Journal of Chemical Technology & Biotechnology. 1999;74(9):835-51.

61.   Castro V, Rodriguez H, Albericio F. Wang Linker Free of Side Reactions. Organic Letters. 2012 2013/01/18;15(2):246-9.

62.   Tae-Kyung Lee J-HC, Jang-Woong Byun, Yoon-Sik Lee. Preparation of MBHA resin by benzotriazole-mediated amidoalkylation. Tetrahedron letters. 2008.

63.   Safer and More Efficient Peptide Coupling Reagent Chemical Synthesis; [cited 2013 19-04-2013].

64.   Michael Vogeser CS. A decade of HPLC - MS/MS in the routine laborator- Goals for further developments. Clinical Biochemistry. 2008;41(9):649-62.

65.   Ali I, Aboul-Enein HY, Singh P, Singh R, Sharma B. Separation of biological proteins by liquid chromatography. Saudi Pharmaceutical Journal. 2010;18(2):59-73.

66.   Schwamborn K, Caprioli RM. MALDI Imaging Mass Spectrometry – Painting Molecular Pictures. Molecular oncology. 2010;4(6):529-38.

59

67.   El-Aneed A, Cohen A, Banoub J. Mass Spectrometry, Review of the Basics: Electrospray, MALDI, and Commonly Used Mass Analyzers. Applied Spectroscopy Reviews. 2009 2009/04/01;44(3):210-30.

68.   Fitzgerald MC, Siuzdak G. Biochemical mass spectrometry: worth the weight? Chemistry & Biology. 1996;3(9):707-15.

69.   Kovtoun S, English R, Cotter R. Mass correlated acceleration in a reflectron MALDI TOF mass spectrometer: an approach for enhanced resolution over a broad mass range. J Am Soc Mass Spectrom. 2002 2002/02/01;13(2):135-43.

70.   J. Kathleen Lewis JWaGS. Matrix-assisted Laser Desorption/Ionization Mass Spectrometry in Peptide abd Protein Analysis. Encyclopedia of Analytical Chemistry.

71.   Sreerama N, Woody RW. Computation and Analysis of Protein Circular Dichroism Spectra. In: Ludwig B, Michael LJ, editors. Methods in Enzymology: Academic Press; 2004. p. 318-51.

72.   Martin SR, Schilstra MJ. Circular Dichroism and Its Application to the Study of Biomolecules. In: Dr. John JC, Dr. H. William Detrich, III, editors. Methods in Cell Biology: Academic Press; 2008. p. 263-93.

73.   C.Price SMKaN. The use of Circular Dichroism in the investigation of Protein Structure and Function. Current Protein and Peptide Science. 2000.

74.   Proteins - Analysis of Structure and Function.   [cited 2013 19-04-2013].

75.   Reddy KVR, Yedery RD, Aranha C. Antimicrobial peptides: premises and promises. International Journal of Antimicrobial Agents. 2004;24(6):536-47.

76.   Lamarre B, Ravi J, Ryadnov MG. GeT peptides: a single-domain approach to gene delivery. Chemical Communications. [10.1039/C1CC13043A]. 2011;47(32):9045-7.